

ORIGINAL
ARTICLE



Synthetic testosterone derivatives modulate rat P2X2 and P2X4 receptor channel gating

Sonja Sivcev*†, Barbora Slavikova‡, Marian Rupert*§, Milorad Ivetic*, Michaela Nekardova‡¶ , Eva Kudova‡ and Hana Zemkova*

**Institute of Physiology, Czech Academy of Sciences, Prague, Czech Republic*

†*Faculty of Science, Charles University, Prague, Czech Republic*

‡*Institute of Organic Chemistry and Biochemistry, Czech Academy of Sciences, Prague, Czech Republic*

§*1st Faculty of Medicine, Charles University, Prague, Czech Republic*

¶*Faculty of Mathematics and Physics, Charles University, Prague, Czech Republic*

Abstract

P2X receptors (P2XRs) are ATP-gated cationic channels that are allosterically modulated by numerous compounds, including steroids and neurosteroids. These compounds may both inhibit and potentiate the activity of P2XRs, but sex steroids such as 17 β -estradiol or progesterone are reported to be inactive. Here, we tested a hypothesis that testosterone, another sex hormone, modulates activity of P2XRs. We examined actions of native testosterone and a series of testosterone derivatives on the gating of recombinant P2X2R, P2X4R and P2X7R and native channels expressed in pituitary cells and hypothalamic neurons. The 17 β -ester derivatives of testosterone rapidly and positively modulate the 1 μ M ATP-evoked currents in P2X2R- and P2X4R-expressing cells, but not agonist-evoked currents in P2X7R-expressing cells. In general, most of the tested testosterone derivatives are more potent modulators than endogenous testosterone. The comparison of chemical structures and whole-cell recordings

revealed that their interactions with P2XRs depend on the lipophilicity and length of the alkyl chain at position C-17. Pre-treatment with testosterone butyrate or valerate increases the sensitivity of P2X2R and P2X4R to ATP by several fold, reduces the rate of P2X4R desensitization, accelerates resensitization, and enhances ethidium uptake by P2X4R. Native channels are also potentiated by testosterone derivatives, while endogenously expressed GABA receptors type A are inhibited. The effect of ivermectin, a P2X4R-specific allosteric modulator, on deactivation is antagonized by testosterone derivatives in a concentration-dependent manner. Together, our results provide evidence for potentiation of particular subtypes of P2XRs by testosterone derivatives and suggest a potential role of ivermectin binding site for steroid-induced modulation.

Keywords: allosteric modulation, ATP, P2XR, testosterone derivatives, purinergic receptors, ivermectin.

J. Neurochem. (2019) 150, 28–43.

Introduction

Extracellular ATP (adenosine-5'-triphosphate) and other nucleotides activate two types of purinergic P2 receptors: ionotropic P2X receptors (P2XRs) and G-protein coupled P2Y receptors (Burnstock, 2006). The family of P2XRs comprises seven subunits (P2X1-7) (North, 2002) that assemble as homo- or hetero-trimers (Nicke *et al.*, 1998). The P2X2R, P2X4R and P2X7R subtypes are the most abundant P2XRs expressed in the brain (Soto *et al.*, 1996; Khakh and North, 2012). Activation of the P2X2R and P2X4R facilitates Ca²⁺ influx (Virginio *et al.*, 1999) and neurotransmitter release (Vavra *et al.*, 2011). The role of P2X4Rs was also confirmed in nociception (Inoue *et al.*, 2004) and in the learning and memory processes (Lorca

et al., 2011). P2X7R is involved in neuropathic pain (Collo *et al.*, 1997) and the release of inflammatory cytokines from activated microglia (Monif *et al.*, 2009). These receptors are homo- or heterotrimeric proteins, with three intersubunit

Received November 6, 2018; revised manuscript received April 24, 2019; accepted April 29, 2019.

Address correspondence and reprint requests to Hana Zemkova; Institute of Physiology, Czech Academy of Sciences, Videnska 1083, 142 20 Prague 4, Czech Republic; E-mail: zemkova@biomed.cas.cz

Abbreviations used: BzATP, 2',3'-O-(benzoyl-4-benzoyl)-ATP; EC50, concentration producing 50% of the maximal response; GABA, γ -aminobutyric acid; HEK, human embryonic kidney; IVM, ivermectin; P2XR, purinergic P2X receptor; RRID, Research Resource Identifier (see scicrunch.org); T, testosterone; TM, transmembrane domain.

ATP binding sites located extracellularly (North, 2002; Hattori and Gouaux, 2012).

The activity of the P2XRs not only depends on the extracellular concentration of agonists but also on the availability of allosteric modulators that enhance or block receptor function (Evans, 2009; Coddou *et al.*, 2011). These modulators include both synthetic compounds (Ase *et al.*, 2015; Muller, 2015) and endogenous modulators, such as calcium (Yan *et al.*, 2011), free fatty acids (Xu *et al.*, 2013) and neurosteroids (De Roo *et al.*, 2003; Codocedo *et al.*, 2009). Neurosteroids are synthesized in the central and peripheral nervous systems, particularly in myelinating glial cells, from cholesterol or steroidal precursors imported from peripheral sources (Baulieu, 1998; Munetsuna *et al.*, 2009; Hojo and Kawato, 2018). Neurosteroids may modify neuronal activity and thereby brain function via a fast, non-genomic action, by acting as allosteric modulators of γ -aminobutyric acid receptors type A (GABA_A) (Harrison and Simmonds, 1984) (Hosie *et al.*, 2006), the nicotinic α 4 β 2 (Paradiso *et al.*, 2001), ionotropic L-glutamate receptors *N*-methyl-D-aspartic acid, NMDA (Sedlacek *et al.*, 2008) or glycine receptors (Ahrens *et al.*, 2008). Little is known about the modulation of P2XRs by neurosteroids, and no studies have analyzed the mechanism and location of neurosteroid action.

Dehydroepiandrosterone, the most abundant neurosteroid in the nervous system (Baulieu, 1998), selectively potentiates the agonist response of endogenous P2X2R expressed in cultured rat sensory neurons (De Roo *et al.*, 2003). A subsequent study revealed that neurosteroids also modulate the activity of P2X4R expressed in HEK293 or oocytes cells. Synthetic steroids, alfaxalone and allopregnanolone, or THDOC (3 α , 21-dihydroxy-5 α -pregnan-20-one), a metabolite of deoxycorticosterone, potentiate while pregnanolone inhibits P2X4R responses at concentrations of 0.1–10 μ M, indicating that neurosteroids likely interact with the P2XR at two distinct modulatory sites (Codocedo *et al.*, 2009). Sex steroids such as 17 β -estradiol or progesterone were reported to be inactive (Codocedo *et al.*, 2009). Here, we tested a hypothesis that testosterone, another 17 β -sex hormone, allosterically modulates activity of P2XRs. We designed and synthesized new derivatives of testosterone to increase the testosterone-induced modulatory effect and analyzed the mechanism of action. Our study is the first to show that 17 β -ester derivatives of testosterone are effective positive allosteric modulators of P2X2R and P2X4R, but not P2X7R, and antagonize the effect of ivermectin (IVM) on P2X4R channel deactivation. These results suggest the involvement of the transmembrane domain in neurosteroid-induced modulation of P2XRs.

Material and methods

Cell cultures and transfection

Experiments were performed using HEK293T cell line (ATCC[®] CRL3216[™], Manassas, VA, USA), which is not listed as a

commonly misidentified cell line. No authentication was performed in our laboratory. Cells were grown in Dulbecco's modified Eagle's medium (Gibco, Rockville, MD, USA, Cat. #41966-029) supplemented with 10% foetal bovine serum (ATCC, Manassas, VA, USA, Cat. #302021) 50 U/mL penicillin and 50 μ g/mL streptomycin (Sigma, St Louis, MO, USA, Cat. #A5955) in a humidified 5% CO₂ atmosphere at 37°C. Passaging was performed for 1–2 months, maximum number of passages was 20. The cells were cultured in 75 cm² plastic culture flasks (Nunc, Rochester, NY, USA, Cat. #156367) for 36–72 h until they reached 80–95% confluence. On the day before transfection, ~150 000 cells were seeded on 35 mm culture dishes (Sarstedt, Newton, NC, USA) and incubated at 37°C for at least 24 h. Transfection was performed using 2 μ g of DNA and 2 μ L of jetPRIME[™] reagent (PolyPlus, Illkirch, France, Cat. #114-15) in 2 mL of Dulbecco's modified Eagle's medium according to the manufacturer's instructions (PolyPlus-transfection). After 24 h of incubation, the transfected cells were mechanically dispersed and re-seeded on 35 mm culture dishes (Corning, New York, NY, USA, Cat. #3294) for 2–6 h prior to recording. For the dye uptake measurements, the transfected cells were plated on 12 mm poly-L-lysine (Sigma, Cat. #P8920-100ML)-coated coverslips (Glaswarenfabrik Karl Hecht KG, Sondheim, Germany, Cat. #1001/12).

DNA constructs

Rat full-length P2X2, P2X4 and P2X7 cDNA subcloned into the bicistronic enhanced green fluorescent protein (EGFP) expression vector, pIRES2-EGFP (Clontech, Mountain View, CA, USA; Research Resource Identifier, RRID:Addgene_43964) was a gift from Dr. S.S. Stojilkovic, NICHD/NIH, Bethesda, MD, USA.

Patch clamp recordings

Currents were recorded in a whole-cell configuration using an Axopatch 200B patch-clamp amplifier (Axon Instruments, Union City, CA, USA) and stored using the pClamp 9.0 software package in conjunction with the Digidata 1322A A/D converter (Molecular Devices, Silicon Valley, CA, USA). Patch electrodes were pulled from borosilicate glass capillaries with firepolished ends, OD = 1.50 mm, ID = 0.86 mm, Length = 8 cm (type GB150F-8P; Science Products GmbH, Hofheim, Germany) using a Flaming Brown horizontal puller (P-87; Sutter Instruments, Novato, CA, USA), and heat-polished to a final tip resistance of 3–5 10 M Ω . The experiments were performed on single cells with an average capacitance of 10 pF, and the membrane potential was held at –60 mV. The access resistance (average 13.8 \pm 2.2 M Ω) was monitored throughout each experiment. Whole-cell recording was always performed with 70–80% series resistance compensation. Only cells with steady state leak current lower than 200 pA were used in subsequent analysis. Patch electrodes were filled with a solution containing 154 mM CsCl, 11 mM EGTA 11, and 10 mM HEPES; the pH was adjusted to 7.2 using 1 M CsOH. The osmolarity of intracellular solution was 293 mOsm. During the experiments, cells were continuously perfused with an extracellular solution containing 142 mM NaCl, 3 mM KCl, 2 mM CaCl₂, 1 mM MgCl₂, 10 mM HEPES and 10 mM D-glucose and adjusted to pH 7.3 using 1 M NaOH. The stock solutions of 20 mM steroids in dimethylsulfoxide were prepared from fresh powder stock every 6 months, and stored at –20°C. Solutions containing ATP and

steroids were applied using the RSC-200 Rapid Solution Changer (Biologic, Claix, France).

EtBr uptake

Cellular accumulation of the fluorescent dye ethidium bromide (EtBr) was examined using an epifluorescent microscope (Olympus BX50WI, Melville, NY, USA). Transfected HEK293 cells plated on glass coverslips were bathed in a normal extracellular solution, imaged using the 409 water immersion objective at 20–25°C and identified by the fluorescence signal of GFP (green fluorescent protein). Changes in fluorescence after EtBr (20 μ M) and ATP (100 μ M) application were recorded using MicroMAX CCD camera (Princeton Instruments; Roper Scientific GmbH, Martinsried, Germany). Hardware control and image analysis were performed using MetaFluor software (Molecular Devices, Downingtown, PA, USA). EtBr was excited at 526 nm and emission was recorded at 605 nm. The average fluorescence signal of 10 cells on each coverslip was calculated and each experiment was repeated 3–16 times.

Animals, brain slices and pituitary cultures

All animal procedures were approved by the Animal Care and Use Committee of the Czech Academy of Sciences (dissection protocol # 67985823). Wistar rats (RRID:RGD_13508588) were obtained from Animal Facility of the Institute of Physiology, Czech Academy of Sciences, approved by Ministry of Environment to use (approval number #56379/2015-MZE-17214), and breed and distribute (approval number #1398/2014-MZE-17214) animals. Breeding pairs of rats were used to produce male and female rats for brain slices and anterior pituitary cell preparations. Rats were housed in cages (42 \times 26 \times 22 cm; 1–2 rats per cage) with wood shavings bedding (LIGNOCEL® 3–4 S; JRS, Rosenberg, Germany), and provided with breeding diet for rats (Altromin, Cat. #1314; Velaz, Prague, Czech Republic) and fresh water ad libitum. Cages were kept in ventilated racks in an acclimated room (at 22 \pm 2°C, with 55% humidity), and lights on from 6 AM to 6 PM. Brains or pituitary glands were removed between 11 AM and 6 PM. Three adult rats were used for brain slices preparations, and 3–6 newborn rats for anterior pituitary cell preparation; in total three pituitary cell culture preparations were performed. Animals of both sexes were used in this study, no exclusion criteria were pre-determined. Euthanasia was performed by decapitation after anaesthesia with isoflurane (Forane, Cat. #B506; AbbVie, Prague, Czech Republic) that does not smell and does not damage epithelium in the respiratory system. No randomization to allocate subject in the study, and no blinding was performed. Study was not pre-registered.

Brain slices containing the supraoptic nucleus (SON) were prepared from 16- to 24-day-old rats (30–35 g weight) as described previously (Vavra *et al.*, 2011). Briefly, brains were removed after decapitation and placed in ice-cold (4°C) oxygenated (95% O₂ + 5% CO₂) artificial cerebrospinal fluid (ACSF). Hypothalamic slices (200- to 300- μ m-thick) were cut with a vibratome (DTK-1000; D.S.K. Dosaka, Japan). Slices were preincubated for at least 1 h at 32–33°C in oxygenated ACSF that contained the following components: 130 mM NaCl, 3 mM KCl, 1 mM MgCl₂, 2 mM CaCl₂, 19 mM NaHCO₃, 1.25 mM NaH₂PO₄, and 10 mM glucose (pH 7.3–7.4; osmolality 300–315 mOsm). During the experiments, slices in recording chamber were submerged in continuously flowing oxygenated ACSF at a

rate of 1–2 mL/min at 20–25°C. Drugs were diluted and applied in a HEPES-buffered extracellular solution. Slices were viewed with an upright microscope (Olympus BX50WI) mounted on a Gibraltar X-Y table (Burleigh) using a water immersion lens (609 and 10 \times) and Dodt infrared gradient contrast (Luigs & Neumann, GmbH, Germany). SON was identified by the position relative to the chiasma opticum (Vavra *et al.*, 2011).

Pituitary cells from 4- to 7-day-old rats (8–10 g weight) were dispersed as described previously (Zemkova and Vanecek, 2000). Briefly, animals were decapitated without anaesthesia, anterior pituitaries were extracted and washed in medium 199 (Gibco, Cat. #22340-020) containing sodium bicarbonate, 10% heat-inactivated foetal bovine serum (Sigma, Cat. #F9665), penicillin (100 U/mL) and streptomycin (100 μ g/mL) (Gibco, Cat. #15140-122), 2 mM glutamine, and treated with papain (Worthington Biochemical, Lakewood, NJ, USA, Cat. #LS003119) for 15 min at 37°C. The cells were mechanically dispersed using a glass pipette (BRAND GmbH, Wertheim, Germany, Cat. # 1780.0150), harvested by centrifugation at 300g for 10 min, and the resulting cell pellet was resuspended in medium 199 and cultured in an air/CO₂ atmosphere at 37°C. For electrophysiology, 0.1–0.2 million cells (in a 200- μ L drop) were plated onto 25-mm glass coverslips coated with 1% poly-L-lysine and cultured in a humidified 5% CO₂ atmosphere at 37°C. Experiments were performed 24–72 h after dispersion.

Patch electrodes used for whole-cell recording from neurons and pituitary cells were filled with an intracellular solution containing: 140 mM KCl, 3 mM MgCl₂, 0.5 mM CaCl₂, 10 mM HEPES, and 5 mM EGTA, pH adjusted to 7.2 with KOH. In current-clamp mode, only cells with resting membrane potential more negative than –40 mV were examined.

Calculations

The concentration-response data points were fitted with the equation $y = I_{max}/[1 + (EC_{50}/x)^h]$, where y is the amplitude of the current evoked by ATP, I_{max} is the maximum current amplitude induced by 100 μ M ATP, EC_{50} is the agonist concentration producing 50% of the maximal response, h is the Hill coefficient, and x is the concentration of ATP (SigmaPlot 2000 v9.01; SPSS Inc., Chicago, IL, USA; RRID:SCR_003210). The kinetics of desensitization or current decay evoked by washout of agonists were fitted by a single exponential function ($y = A_1 \exp(-t/s)$) or by the sum of two exponentials ($y = A_1 \exp(-t/s_1) + A_2 \exp(-t/s_2)$) using the program pClamp 10 (Molecular Devices), where A_1 and A_2 are relative amplitudes of the first and second exponentials, and s_1 and s_2 are the time constants. The derived time constants for deactivation and desensitization were labelled as s_{off} and s_{des} , respectively. Weight desensitization constant was calculated as $y = [(A_1 \times s_1) + (A_2 \times s_2)] / (A_1 + A_2)$. No sample calculation was performed, no test for outliers and no assessment of the normality of data was carried out; study was exploratory.

Statistical analysis

All numerical values in the text are reported as the mean SEM. Comparisons between two groups were performed by Student's unpaired t test ($*p < 0.01$ and $*p < 0.05$). In the case of ethidium uptake, statistical comparison of multiple groups was made by using one-way ANOVA followed by Tukey's post hoc test in SigmaStat 2000 v9.0 (Systat Software, San Jose, CA, USA; RRID:SCR_

010285), for comparison to a single control. The 'n' indicates number of cells throughout the study, if not otherwise stated.

Chemicals and synthesis of new testosterone derivatives

Based on preliminary data, we designed and synthesized new derivatives of testosterone in order to increase the steroid-induced modulatory effect: T-butyrate, T-valerate, T-caproate, T-isovalerate, T-methylhexanoate, T-methylbutyrate, T-perfluorobutyrate, T-pivalate and T-hexanoate. These compounds have been prepared from commercially available testosterone via esterification reaction at position C-17 of the D-ring of the steroid (Supplementary information, Scheme S1). Custom-made materials will be shared upon reasonable request. Ivermectin (IVM; Cat. #18898) and all other chemicals were from Sigma (St. Louis, MO, USA).

Results

Testing of the abilities of new testosterone derivatives to modulate the function of P2XRs

Electrophysiological whole-cell recordings from HEK293 cells transfected with P2X2R or P2X4R were performed using a short (1–3 s) application of 1 μ M ATP in the presence and absence of 3 μ M steroid. Most testosterone derivatives (Fig. 1) potentiated ATP-induced responses, without

differences between P2X2R and P2X4R (Fig. 2a, upper traces). Whole-cell recordings from HEK293 cells expressing rat P2X7R and stimulated with 5–10 s applications of 30 μ M 2',3'-O-(benzoyl-4-benzoyl)-adenosine 5'-triphosphate (BzATP), an artificial but potent agonist of P2X7Rs, revealed that this receptor subtype was insensitive to 30 μ M T-butyrate (104 \pm 4%, n = 5; Fig. 2a, lower trace).

The comparison of chemical structures and whole-cell recordings revealed that interactions of testosterone analogues with the P2XRs depend on lipophilicity (estimated as logP; Table S1) and the length of the linear alkyl chain at position C-17 (Fig. 2b). Testosterone derivatives with alkyl chains containing 4 or 5 carbons were the most efficient (compound 4, T-butyrate, P2X2R: 145 \pm 9%, n = 4, p < 0.01; P2X4R: 148 \pm 4%, n = 10, p < 0.01; compound 5, T-valerate, P2X2R: 154 \pm 13%, n = 6, p < 0.01; P2X4R: 149 \pm 8%, n = 12, p < 0.01). Both shorter and longer substituents exhibited lower potentiating effects, and testosterone and compounds 2 and 8 were almost completely inactive (Fig. 2b). Branching (Fig. 2c) or miscellaneous modifications (Fig. 2d) of the alkyl chain did not further increase the potentiating effect, with the exception of the perfluorinated analogue that selectively enhanced P2X2R

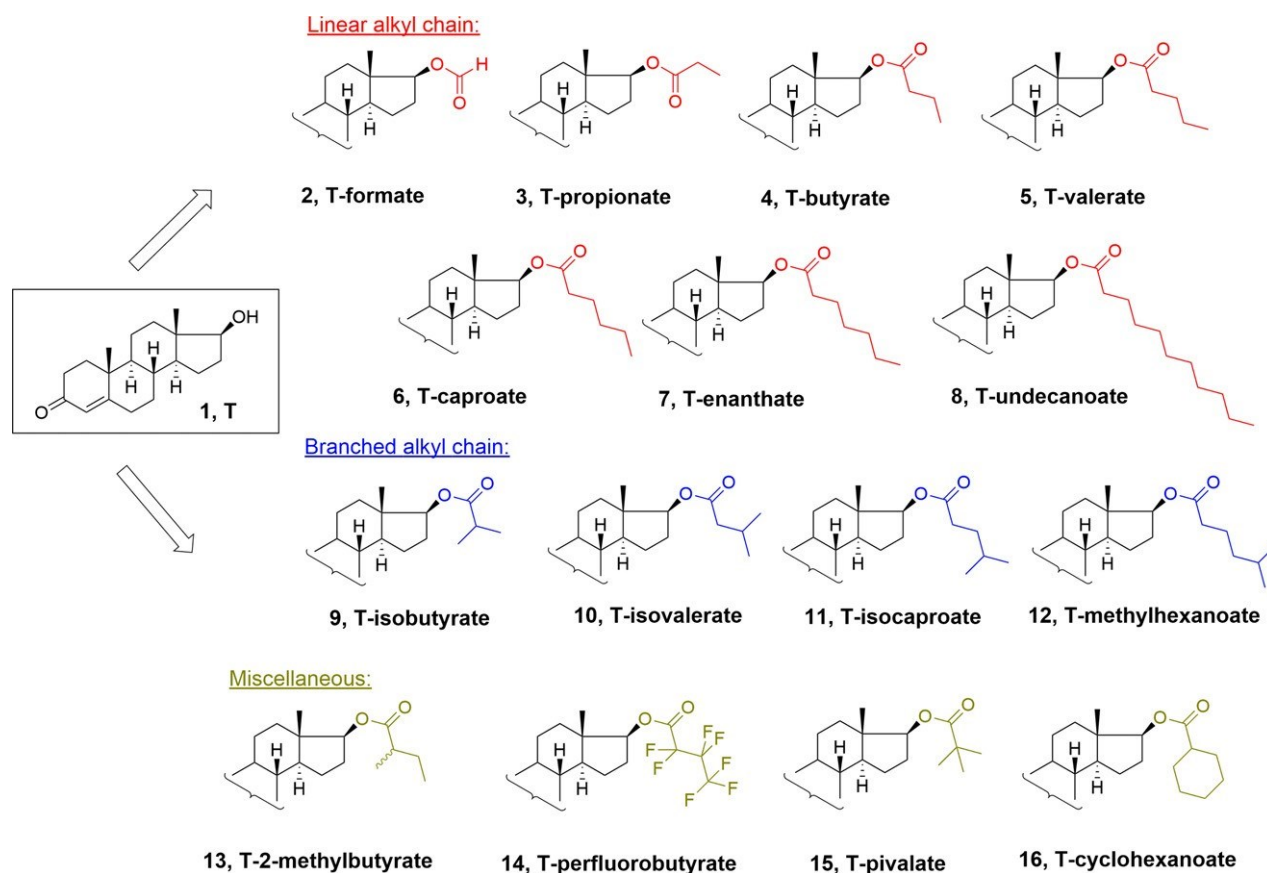


Fig. 1 Testosterone derivatives modified at position C-17 via the ester bond. Three types of modifications of the alkyl chain at position C-17 on the D-ring of testosterone have been tested in this study: linear, branched or miscellaneous modifications

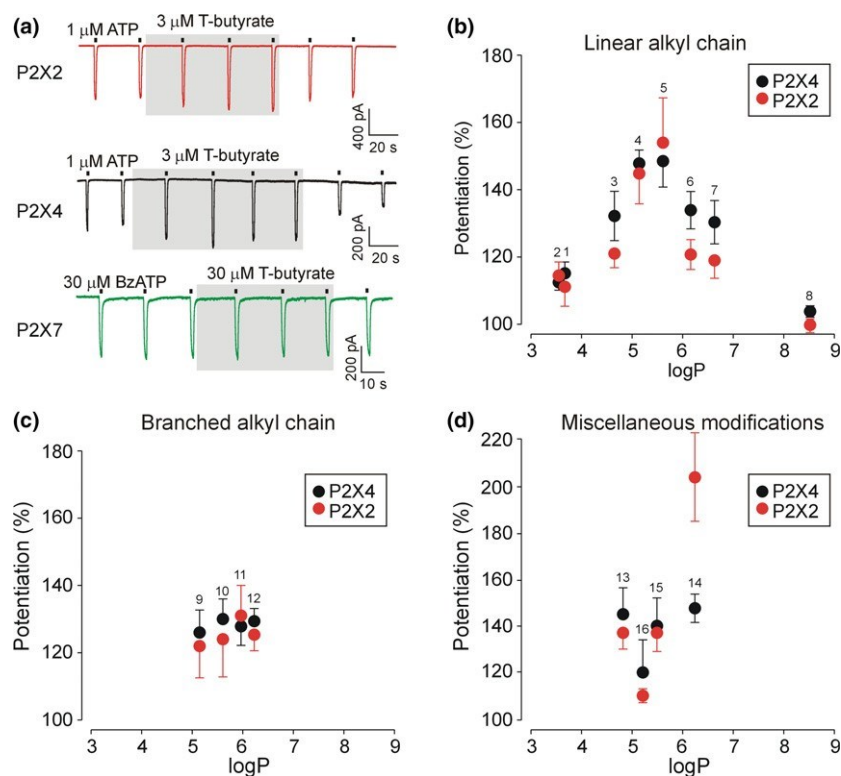


Fig. 2 Potentiating effect of testosterone derivatives on agonist-induced currents in HEK293 cells expressing rat P2X2R, P2X4R and P2X7R. (a) Representative recordings from cells transfected with the P2X2R (red), P2X4R (black) or P2X7R (green). T-butyrate (3 or 30 μ M) application potentiated the peak amplitude of currents induced by repetitive stimulation with 1 μ M ATP (2-s pulse applied every 20 s) in cells expressing P2X2R and P2X4R, but had no effect on BzATP-induced current in P2X7R-expressing cells. In this and other figures, grey areas indicate the testosterone derivative application and black bars above the traces indicate the ATP application. (b–d) Dependence

activity (compound 14, T-perfluorobutyrate, P2X2R: 203 \pm 18%, $n = 4$; P2X4R: 147 \pm 6%, $n = 5$), indicating that steroid binding site is not completely conserved in P2X2R and P2X4R; this effect was not investigated further. Epi-testosterone, 17 α -OH testosterone, (10 μ M) was less efficient modulator compared to testosterone (10 μ M) in both receptor types (epi-testosterone, P2X2R: 102 \pm 0.6%, $n = 4$; P2X4R: 105 \pm 2.2%, $n = 4$; testosterone, P2X2R: 122 \pm 11%, $n = 3$; P2X4R: 134 \pm 6%, $n = 3$).

These results revealed that 17 β -ester derivatives of testosterone selectively potentiate P2X2R and P2X4R, but not P2X7R, and derivatives with alkyl chains containing 4 or 5 carbons are the most efficient.

Concentration-dependent potentiating effects of testosterone derivatives on P2X4R

We measured the amplitude of 1 μ M ATP-induced P2X4R responses in the presence of various concentrations (1, 3, 10

or 30 μ M) of steroids to further characterize the potentiating effects of testosterone and its derivatives (Figs. 3 and Table S2); concentrations greater than 30 μ M were not tested due to the poor solubility of some compounds at these concentrations. Testosterone and testosterone derivatives produced concentration-dependent potentiating effects without eliciting changes in the basal current of HEK293 cells (Fig. 3a and 3). The concentration analysis showed that testosterone derivatives with linear alkyl chains containing a C4 or C5 ester moiety at position C-17 of the D-ring were more efficient than compounds with shorter (C2 or C3) or longer (C6–C8) linear chains at all concentrations tested (Fig. 3c and 3), and the potentiation was not enhanced by branching or any other modifications (Fig. 3e and 3). These data also revealed that most testosterone derivatives (compounds 2–7 and 9–16) exhibited greater potentiating effects than testosterone alone (compound 1).

or 30 μ M) of steroids to further characterize the potentiating effects of testosterone and its derivatives (Figs. 3 and Table S2); concentrations greater than 30 μ M were not tested due to the poor solubility of some compounds at these concentrations. Testosterone and testosterone derivatives produced concentration-dependent potentiating effects without eliciting changes in the basal current of HEK293 cells (Fig. 3a and 3). The concentration analysis showed that testosterone derivatives with linear alkyl chains containing a C4 or C5 ester moiety at position C-17 of the D-ring were more efficient than compounds with shorter (C2 or C3) or longer (C6–C8) linear chains at all concentrations tested (Fig. 3c and 3), and the potentiation was not enhanced by branching or any other modifications (Fig. 3e and 3). These data also revealed that most testosterone derivatives (compounds 2–7 and 9–16) exhibited greater potentiating effects than testosterone alone (compound 1).

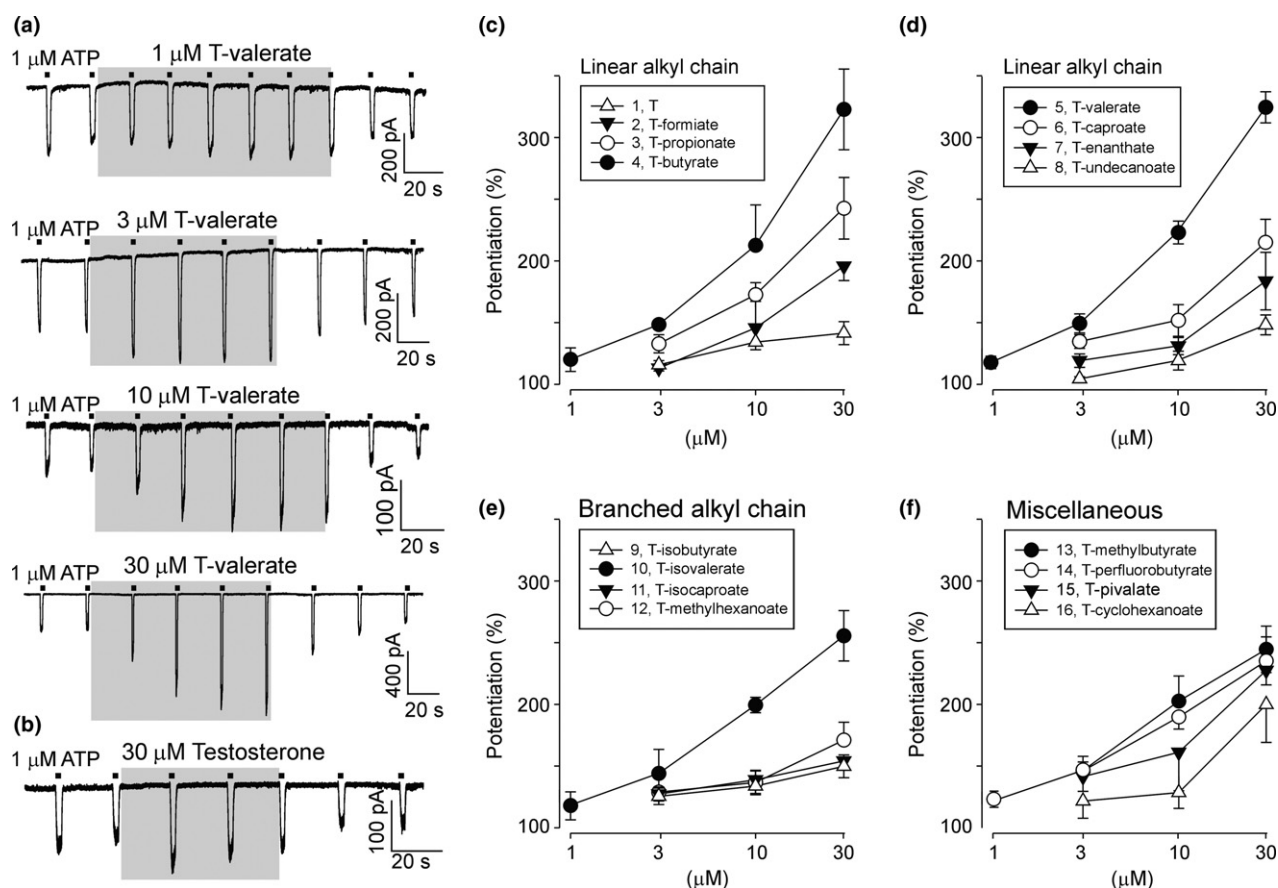


Fig. 3 Concentration-dependent effects of testosterone and testosterone derivatives on P2X4R currents. (a) Representative recordings showing the potentiating effect of T-valerate (1, 3, 10 and 30 μM) on P2X4R responses stimulated with 1 μM ATP. (b) Example recording showing potentiating effect of 30 μM testosterone on 1 μM ATP-induced P2X4R response. (c and d) Potentiation by compounds 1–8 (in % of control) that differ in the length of the linear alkyl chain. Experiments were performed on cells stimulated with 1 μM ATP in the

presence or absence of 1, 3, 10 or 30 μM steroid. (e) Concentration-dependent effects of compounds 9–12 containing the branched alkyl chain. (f) Concentration-dependent effect of compounds 13–16 containing miscellaneous modifications. Numbers and names of compounds are shown in boxes. The threshold concentration, 1 μM , is shown in each panel only for the most effective steroids. Data points represent the mean SEM; $n = 4$ –35 cells from 3 to 12 passages per concentration.

Testosterone derivatives increase the sensitivity of P2X2R and P2X4R to ATP

Whole-cell recordings from P2X4R-transfected cells stimulated with various concentrations of ATP (Fig. 4a) showed that preincubation with 30 μM steroid shifted the ATP concentration-response curve to the left, reduced the ATP concentration producing a half-maximal potentiating effect (EC_{50}) by 3.5-fold (control $EC_{50} = 2.4 \pm 0.4 \mu\text{M}$; T-butyrate $EC_{50} = 0.7 \pm 0.1 \mu\text{M}$; $p < 0.01$; Fig. 4d) and slightly increased the maximum current amplitude at saturating ATP concentrations (to approximately 120%), but this effect was not statistically significant (control: $1.8 \pm 0.18 \text{ nA}$; T-butyrate: $2.1 \pm 0.17 \text{ nA}$; $n = 5$, $p > 0.05$). The ATP concentration-response curve for P2X2R was also leftward shifted and EC_{50} was reduced by 1.7-fold (control $EC_{50} = 3.2 \pm 0.7 \mu\text{M}$; T-butyrate $EC_{50} = 1.9 \pm 0.4 \mu\text{M}$; $p < 0.05$; Fig. 4e), but the maximum current amplitude at

saturating ATP concentrations was not affected (Fig. 4b and 4e). The BzATP concentration-response curve for P2X7R was not displaced and 30 μM T-butyrate had no effect on maximum current amplitude (Fig. 4c and 4f) or the time course of secondary current growth and receptor deactivation (Figure S1). Thus, testosterone derivatives allosterically potentiate P2X2R and P2X4R responses predominantly by increasing the sensitivity of the receptor to the agonist.

Testosterone derivatives reduce the rate of P2X4R desensitization and accelerate resensitization

P2X4R becomes moderately desensitized within less than 10 seconds and recovery from complete desensitization takes between 10 and 15 min (North, 2002). We examined the effect of T-butyrate (30 μM) on the rate of P2X4R desensitization using a prolonged (40 s) application of 100 μM ATP. In the absence of steroid, P2X4R was almost

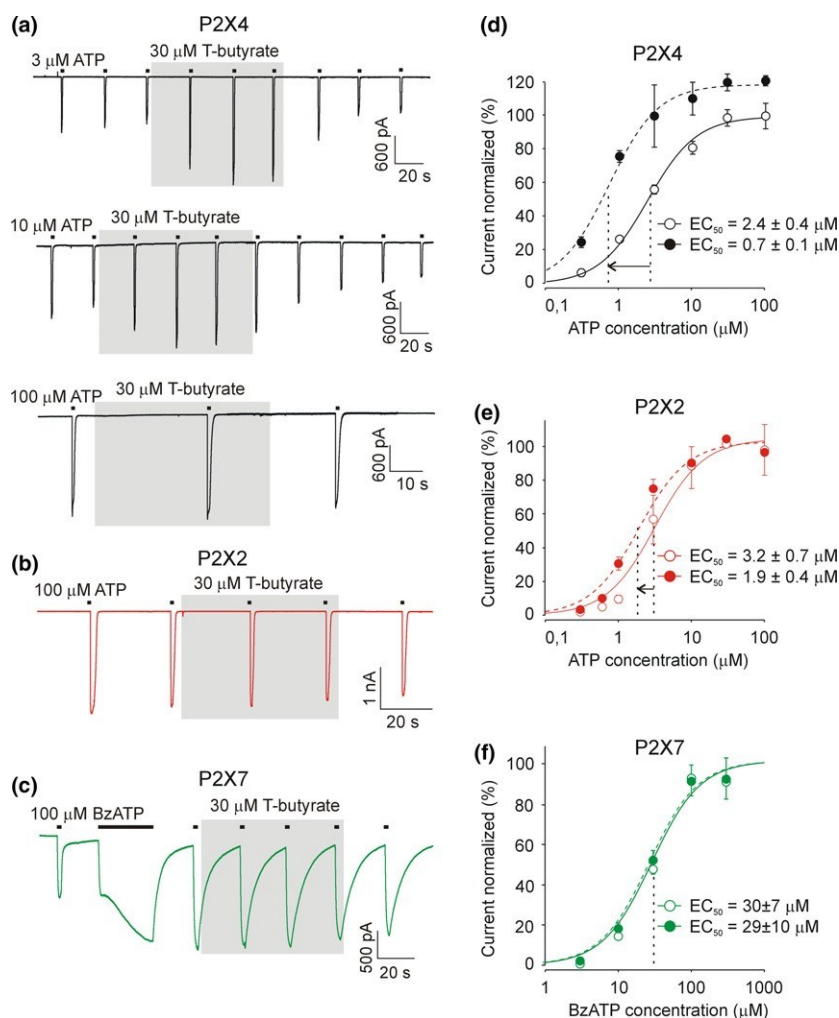


Fig. 4 Effect of T-butyrate on the agonist concentration-response curve and the maximum peak current amplitude. (a) Representative recordings showing the potentiating effect of 30 μM T-butyrate on peak P2X4R responses to 3, 10 and 100 μM ATP. (b) Representative recording showing no effect of T-butyrate on peak P2X2R response to 100 μM ATP. (c) Representative recording showing no effect of T-butyrate on peak P2X7R response to 100 μM BzATP. (d–f) Concentration-dependent effects of agonist on the peak amplitude of current in the absence (open circles) and presence (closed circles) of 30 μM T-butyrate for P2X4R (d), P2X2R (e) and P2X7R (f). The vertical dotted lines represent the ATP concentration producing the 50% maximal response, the numbers represent the mean EC_{50} values, and the arrow indicates the leftward shift of the ATP concentration-response curve in the presence of testosterone butyrate. The Hill coefficient was fixed to 1.3, a value obtained for P2X4R by fitting the curve in the absence of steroid. Data points represent the mean \pm SEM; $n = 5$ –17 cells from three to six passages per concentration.

completely desensitized (Fig. 5a, left). In the presence of steroid, the desensitization time constant (s_{des}) increased (Fig. 5a, right) by approximately twofold (control, $s_{\text{des}} = 9.0 \pm 0.6$ s, $n = 3$; T-butyrate, $s_{\text{des}} = 21.5 \pm 4.2$ s, $n = 3$; $p < 0.01$) and the non-desensitized plateau current increased from $3.8 \pm 0.8\%$ ($n = 4$) to $26.6 \pm 2.0\%$ ($n = 4$; $p < 0.01$) of the initial peak current amplitude (Fig. 5e).

When two or more consecutive ATP pulses were delivered in the absence of steroid, no recovery of the peak current response was observed after 30 or 60 s of washout (Fig. 5b). In the presence of 3 μM T-butyrate for 30 s, the third peak amplitude recovered to $227 \pm 19\%$ ($n = 6$) of the second peak amplitude (Fig. 5c and 5). This effect was even higher when steroid was applied immediately after the first pulse (Fig. 5d). Based on these results, testosterone derivatives reduce the rate of P2X4R desensitization and accelerate the recovery of the desensitized peak current response. A similar effect was observed for IVM, a P2X4R-specific allosteric modulator (Khakh *et al.*, 1999; Mackay *et al.*, 2017).

Testosterone derivatives support pore opening in the P2X4R

The ability to open a dye permeable pore may be a common characteristic of P2XRs (Karasawa *et al.*, 2017), and electrophysiological experiments showed that IVM is able to potentiate the formation of a large pore in P2X4R (Zemkova *et al.*, 2015; Mackay *et al.*, 2017). We measured the uptake of ethidium bromide (EtBr) by HEK293 cells expressing the P2X4R in the presence and absence of T-valerate or IVM to test the hypothesis that testosterone derivatives also potentiate large pore opening. In the control experiment, the application of 100 μM ATP stimulated rapid EtBr accumulation that was detectable within 10–7 s and was peaked at 50 s after agonist application (Fig. 6a). In cells treated with T-valerate (30 μM) or IVM (3 μM), the rate of ATP-stimulated EtBr uptake was faster than the control, and maximum fluorescence signal measured at 50 s after agonist application increased to $120 \pm 9\%$ ($n = 4$; $p < 0.05$) and $133 \pm 20\%$ ($n = 3$; $p < 0.01$), respectively, (Fig. 6b). Combined with the electrophysiological measurements, these data

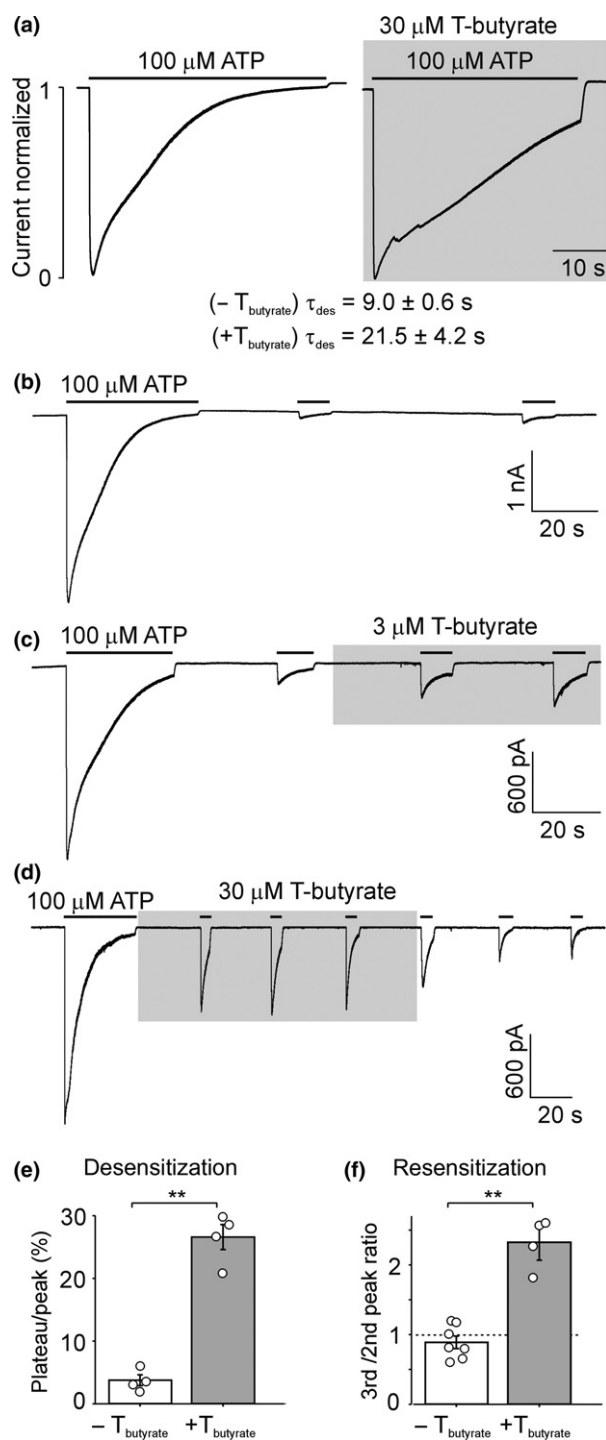


Fig. 5 Effect of T-butyrate on the desensitization properties of P2X4R. (a) Comparison of the time courses of currents induced by prolonged (40 s) application of 100 μM ATP in the presence (right) and absence (left) of 30 μM T-butyrate. The desensitization time constant (τ_{des}) was measured by fitting the curve to a monoexponential (in the presence of steroid) or biexponential (in the absence of steroid) functions; desensitization time constants derived from biexponential fitting were weight. The data are presented as the means \pm SEM from eight and seven cells, respectively. (b) Representative recording showing the desensitization of the peak P2X4R current induced by 100 μM ATP in control experiments. Practically no recovery was observed when the ATP pulse was repeatedly applied after 30 and 60 s of washout. (c and d) Accelerated recovery from the P2X4R desensitization was induced by the application of 3 or 30 μM T-butyrate. (e) Summary histogram showing the desensitization (plateau-to-peak ratio) in the presence (grey column) and absence (white column) of steroid. Data are presented as the mean SEM with a scatterplot of the individual data points ($n = 4$ cells from four passages). (f) Summary histogram showing the recovery from desensitization (the 2nd-to-3rd peak ratio) in the presence (grey column) and absence (white column) of steroid. Data are presented as the mean SEM with a scatterplot of the individual data points ($n = 4-7$ cells from four passages). The statistical significance was estimated using unpaired t-test, $p < 0.01$ (**).

involvement of the allosteric binding site for IVM in steroid-induced P2X4R potentiation. When 3 μM IVM was applied in the absence of steroid, the amplitude of the 1 μM ATP-stimulated current increased 5.9 \pm 0.6-fold ($n = 16$, $p > 0.01$; Fig. 7a and 7b). When IVM was applied in the presence of steroid, which alone increases the amplitude of ATP-stimulated current by 2.1 \pm 0.3-fold ($n = 27$, $p > 0.01$; Fig. 3d), the amplitude of the ATP response was further increased by 5.2 \pm 0.9-fold ($n = 6$; $p > 0.01$ Fig. 7b and 7). On the other hand, the application of T-valerate in the presence of IVM had a tendency to reduce the potentiating effect of IVM (4.0 \pm 0.8; $n = 12$, Fig. 7c and 7e). However, this effect was not significant ($p = 0.55$).

We next evaluated the deactivation properties of P2XRs and measured time constant (s_{off}), which was obtained by fitting the current decay evoked by 1 μM ATP removal. In the absence of T-valerate, the deactivation of P2X2R and P2X4R proceeded with a time constant of 197 \pm 23 ms ($n = 5$) and 105 \pm 3 ms ($n = 15$), respectively. In the presence of T-valerate (3 μM) for 1–2 min, the deactivation time constant did not change: 205 \pm 23 ms ($n = 5$) and 103 \pm 4 ms ($n = 20$) for P2X2R and P2X4R, respectively; 30 μM steroid had slight effect (P2X4R, $s_{off} = 218 \pm 16$ ms; $n = 8$; Fig7f). Figure S1 shows that T-butyrate has no effect on deactivation of P2X7R.

When 3 μM IVM was applied in the absence of steroid for 30–60 s, the time constant of P2X4R deactivation increased to 4.79 \pm 0.60 s ($n = 25$; Fig. 7a and 7). When IVM was applied in the presence of T-valerate (3 μM), the

provide evidence that testosterone derivatives potentiate the activity of P2X4R to open a large pore, similarly to IVM.

Antagonizing effect of testosterone derivatives on the effect of IVM on P2X4R deactivation

We monitored the effect of IVM in the presence and absence of T-valerate (10 μM) to explore the possible

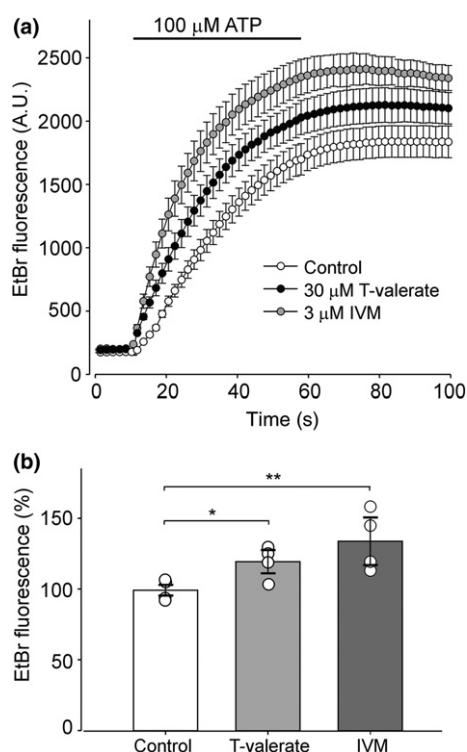


Fig. 6 Potentiation of ATP-stimulated ethidium bromide (EtBr) uptake by the preapplication of testosterone derivatives or ivermectin. (a) Representative fluorescent measurement of ethidium accumulation by HEK293 cells expressing P2X4R in a control experiment (open symbols) and in the presence of 30 μM T-valerate (black) or 3 μM IVM (gray). EtBr accumulation was triggered by 100 μM ATP (horizontal bar) and dye uptake was determined as the amplitude of the EtBr signal 50 s after the ATP application. Signals from 5 to 10 cells were averaged. The intensity of light emission was measured every 1–2 s; for clarity, some data points have been omitted. A.U., arbitrary units. (b) Summary graph with ATP-stimulated EtBr fluorescence (in % of control) in the presence of 30 μM T-valerate (light gray column) or 3 μM IVM (dark gray column). Data are presented as the mean \pm SEM with a scatterplot of the individual data points ($n = 4$, $n =$ number of experiments which equals number of cell passages); statistical significance was estimated by using one-way ANOVA followed by Tukey's post hoc test, $p < 0.05$ (*) and $p < 0.01$ (**).

deactivation time constant only increased to 2.3 \pm 0.75 s ($n = 5$; Fig. 7d and 7). The antagonizing effect of T-valerate was concentration-dependent; in the presence of 10 μM steroid, the IVM-induced deactivation time constant was reduced to 0.85 \pm 0.13 s ($n = 17$; Fig. 7b and 7). Testosterone alone (30 μM) did not significantly reduce the effect of IVM on deactivation ($s_{\text{off}} = 3.93 \pm 0.95$ s; $n = 3$; not shown).

Thus, the allosteric binding site on P2X4R is more accessible to IVM in the absence of T-valerate than in its presence. Based on our data, testosterone derivatives bind to a position located near the IVM binding site and might displace IVM from its binding pocket.

Potentiation of endogenously expressed P2XRs in pituitary cells and hypothalamic neurons

For comparison with endogenously expressed receptors, the effect of testosterone derivatives was tested on native P2XRs in primary cultures of anterior pituitary cells and hypothalamic SON neurons in rat brain slices (Fig. 8). ATP-induced currents were recorded from pituitary gonadotrophs that exclusively express P2X2R (Zemkova *et al.*, 2006) and pituitary lactotrophs that express the P2X4R subtype (Zemkova *et al.*, 2010). SON expresses both receptor subtypes on neuronal somata and terminals (Vavra *et al.*, 2011). The preapplication of T-valerate (3–30 μM) increased the amplitude of ATP (30–100 μM)-evoked currents both in gonadotrophs (Fig. 8a) and lactotrophs (Fig. 8b), as well as in non-identified pituitary cells (Fig. 8c, upper trace) on average to 152 \pm 13% ($n = 12$, Fig. 8e). Treatment of pituitary lactotrophs with T-valerate also increased the P2X4R desensitization time constant (Fig. 8b) by 2.6-fold (control, $s_{\text{des}} = 6.0 \pm 1.4$ s; T-valerate, $s_{\text{des}} = 16.1 \pm 1.8$ s, $n = 4$; $p < 0.01$, Fig. 8f, left). SON neurons in slices respond to the ATP application with a somatic current and increases in the frequency of spontaneous postsynaptic currents (Vavra *et al.*, 2011). A treatment with 3 μM T-butyrate potentiated these effects of ATP in three of five neurons tested (five slices from three rats; Fig. 8d).

All subtypes of anterior pituitary cells express similar subtype of GABA_A receptor (Zemkova *et al.*, 2008). For comparison with other endogenously expressed ligand-gated receptor channels, the effect of testosterone derivatives on GABA-induced responses in non-identified pituitary cells was subsequently tested (Fig. 8c, lower trace). In contrast to ATP-induced responses, the amplitude of the GABA-evoked current was reduced on average to 62 \pm 2.6% ($n = 19$, Fig. 8e) and the GABA_A receptor desensitization time constant to 45 \pm 5.7% (control, $s_{\text{des}} = 9.0 \pm 1.2$ s; T-valerate, $s_{\text{des}} = 3.8 \pm 0.6$ s, $n = 7$; $p < 0.01$, Fig. 8f). Thus, testosterone derivatives selectively potentiate endogenously expressed P2X2R and P2X4R, but inhibit GABA_A receptors.

Discussion

The results of our study show that 17 β -ester derivatives of testosterone selectively interact with particular subtypes of P2XRs, namely, P2X2R and P2X4R, but not P2X7R. These compounds are not able to substitute as ligands binding to the orthosteric binding site, but may modulate their affinity and possibly displace IVM from the allosteric binding site on P2X4R.

Dehydroepiandrosterone potentiates P2X2R in cultured rat sensory neurons (De Roo *et al.*, 2003), and alfaxalone, allopregnanolone and 3 α ,21-dihydroxy-5 α -pregnan-20-one (THDOC) potentiate rat P2X4R expressed in HEK293 or oocytes cells at concentrations of 0.1–10 μM (Codocedo *et al.*, 2009). Endogenous sex steroids, progesterone or 17 β -

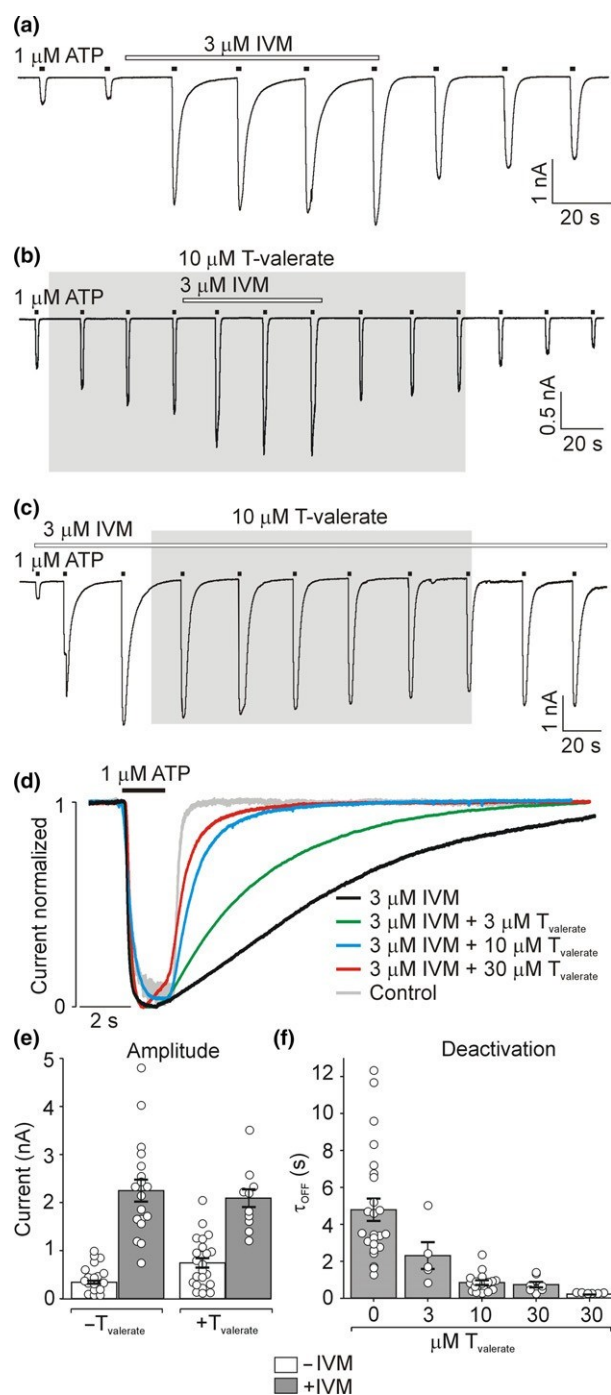


Fig. 7 Effect of T-valerate on ivermectin (IVM)-induced delay in P2X4R deactivation. (a) Example recording showing the effects of 3 μM IVM on 1 μM ATP-induced P2X4 current amplitude and channel deactivation. The horizontal open bar indicates the time of IVM application, and 2-s pulses of ATP are indicated by black bars above the traces. (b) Example recording showing the inhibitory effect of pretreatment with 10 μM T-valerate (gray area) on IVM-induced delay in deactivation. (c) Same as (b) but T-valerate was applied in the presence of IVM. (d) Expanded recordings of currents induced by the washout of 1 μM ATP in the presence of 3 μM IVM and several concentrations of T-valerate (3, 10 and 30 μM). Control trace was recorded in the absence steroid and IVM (gray trace). (e) Summary histograms showing the effects of 10 μM T-valerate on the 1 μM ATP-induced current amplitude in the presence (gray columns) and absence (white columns) of IVM. Data are presented as the mean SEM with a scatterplot of the individual data points ($n = 10-23$ cells from five to eight passages). (f) Summary histograms show the effects of 3, 10 or 30 μM T-valerate on the deactivation time constant (τ_{OFF}) of 1 μM ATP-induced current in the presence (gray columns) and absence (white column) of IVM. Data are presented as the mean SEM with a scatterplot of the individual data points ($n = 5-25$ cells from three to eight passages per concentration).

the 3 α -hydroxyl group, such as alfaxalone or THDOC, directly gate P2X4R and open the channel pore in the absence of agonist at concentrations 10- to 30-fold higher than those required to modulate ATP-evoked currents (Codocedo *et al.*, 2009). We did not observe this effect with 30 μM 17 β -ester derivatives of testosterone. These findings may be interpreted to indicate that modulatory effects related to structurally specific sites of the steroid molecule are likely mediated by different mechanisms.

The potentiating effect of T-butyrate or T-valerate was due to a steroid-induced increase in the sensitivity of the receptor to ATP, rather than to increased efficacy of the agonist. The small increase in the 100 μM ATP-evoked response mediated by P2X4R was apparently due to steroid-induced inhibition of desensitization and accelerated resensitization. Thus, upon binding, testosterone analogues acting as allosteric modulators may change the P2XR protein conformation and subsequently alter the binding of orthosteric ligands, enhancing receptor function. A similar mechanism has been suggested for IVM, a P2X4R-specific allosteric modulator (Khakh *et al.*, 1999; Priel and Silberberg, 2004; Jelinkova *et al.*, 2006; Mackay *et al.*, 2017). Testosterone derivatives and IVM also potentiated ATP-stimulated ethidium uptake by HEK293 cells expressing the P2X4R, further showing that these compounds share common mechanisms of action.

However, some differences also exist between the actions of testosterone derivatives and IVM. First, we observed a clear correlation between the potentiating effect on the P2X2R and P2X4R responses, suggesting that the binding site for testosterone analogues is well conserved among these two types of P2XRs. On the other hand, IVM only

estradiol, did not significantly alter the ATP-evoked P2X4 responses in HEK293 cells or oocytes cells (Codocedo *et al.*, 2009). Also native testosterone (3 μM) did not effectively potentiate P2XRs in the present study. However, derivatives of testosterone with a 4–5 carbon alkyl chain at position C-17 of the steroid D-ring potentiate both P2X2R and P2X4R, indicating that the modulatory effects of steroids might rely on different parts of the molecule. Neurosteroids containing

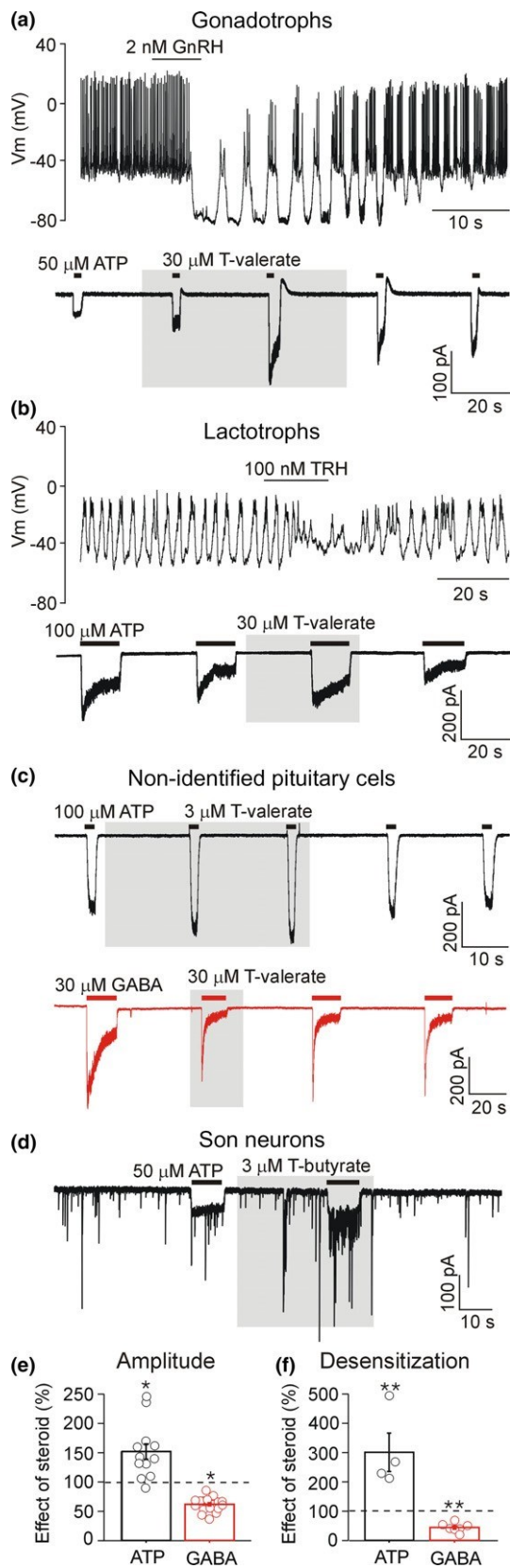


Fig. 8 Potentiating effects of testosterone analogues on endogenously expressed P2XRs in anterior pituitary cells and hypothalamic neurons. (a) Potentiation of P2X2R in pituitary gonadotrophs. On top example of current clamp whole-cell recording of action potentials stimulated by gonadotropin releasing hormone (GnRH) that was used to identify gonadotrophs. GnRH-evoked membrane potential (V_m) oscillations that are mediated by activation of oscillatory Ca^{2+} -dependent K^+ current. Below application of T-valerate (30 μ M) potentiated the ATP (50 μ M)-stimulated response mediated by native P2X2R (Zemkova et al., 2006) in cell voltage clamped at -60 mV. (b) Potentiation of P2X4R in pituitary lactotrophs. On top example current clamp recording from pituitary lactotrophs identified according to the thyrotropin releasing hormone (TRH)-stimulated response. Below, application of T-valerate (30 μ M) in cell voltage clamped at -60 mV potentiated the amplitude and reduced rate of desensitization of the ATP (100 μ M)-stimulated response mediated by native P2X4R (Zemkova et al., 2010). (c) On top potentiating effect of 3 μ M T-valerate on the 100 μ M ATP-induced current in non-identified anterior pituitary cell. Below inhibitory effect of 30 μ M T-valerate and accelerated desensitization of γ -aminobutyric acid (GABA) (50 μ M)-induced current in non-identified pituitary cell. (d) Representative recording from a SON neuron in rat brain slices showing the potentiation effect of 3 μ M T-butyrate on the 50 μ M ATP-induced inward current and frequency of spontaneous postsynaptic currents (example response from six similar cells from three animals). (e) Summary graphs showing effects of testosterone derivatives on amplitude of ATP- and GABA-induced current in pituitary cells. Data are presented as the mean \pm SEM with a scatterplot of the individual data points (ATP, $n = 12$ cells from three cell culture preparations; GABA, $n = 19$ cells from three cell culture preparations). (f) Same as (e) but monoexponential and biexponential desensitization fitting of ATP- and GABA-induced current, respectively. Data are presented as the mean \pm SEM with a scatterplot of the individual data points (ATP, $n = 4$ cells from three cell culture preparations; GABA, $n = 7$ cells from three cell culture preparations). Significant differences between responses in the presence and absence of testosterone derivatives were estimated using the unpaired t -test (* $p < 0.05$; ** $p < 0.01$).

potentiates the P2X4R subtype (Khakh *et al.*, 1999). Second, pre-treatment with IVM highly significantly prolongs the deactivation of P2X4R after the removal of agonist (up to 60-fold) (Jelinkova *et al.*, 2006), while no effect on deactivation was observed after the application of testosterone derivatives.

In the P2X4Rs and other ligand-gated ion channels, the allosteric modulatory site for IVM is located in the transmembrane domain and is formed by an inter-subunit hydrophobic pocket (Jelinkova *et al.*, 2006; Lynagh and Lynch, 2012; Latapiat *et al.*, 2017), reviewed by (Zemkova *et al.*, 2014; Huang *et al.*, 2017). The finding that T-valerate antagonizes the effect of IVM on P2X4R deactivation might indicate that the allosteric modulatory site for testosterone derivatives is located within the TM domain, partially overlapping with the IVM binding pocket in P2X4R. We can also speculate that the conserved binding of testosterone derivatives causes conformational changes that affect receptor-specific IVM binding; this possibility needs further investigation.

The P2X7R is known to be modulated by endogenous cholesterol that inhibits channel activity by binding to the transmembrane helices, and drugs that interact with the cholesterol binding site of the P2X7R may reduce the inhibitory effect of cholesterol (Murrell-Lagnado, 2017). Our data show that testosterone derivatives are not able to potentiate agonist-stimulated current or shift the concentration-response curve for P2X7R, indicating that these compounds cannot interact with the cholesterol binding site.

Potentiating effects of testosterone and testosterone derivatives were observed at relatively high concentrations (1–30 μM) that are unlikely to be reached locally under physiological conditions (Baulieu, 1998; Rupprecht and Holsboer, 1999), but might be achieved during treatment with anabolic steroids containing synthetic testosterone derivatives, before they are cleaved in the plasma by esterases to provide testosterone. Anabolic steroids regulate the transcription of target genes that control the accumulation of DNA required for skeletal muscle growth, and stimulate the brain through their diverse effects on various central nervous system neurotransmitters via a fast, non-genomic action (Ganesan and Pellegrini, 2018). The application of anabolic steroids might induce emotional lability, major mood disorders, anosmia, headache, depression, nervousness, body pain, violence insomnia and aggressive behaviour (Ganesan and Pellegrini, 2018). After one dose of anabolic steroids, 750 mg, administered as oral pills, injections, creams or topical gels, and skin patches, the levels of testosterone derivatives in plasma might increase up to 10 μM , a sufficient concentration to potentiate endogenously expressed P2X2R or P2X4R (Fig. 8). Thus potentiation of P2XRs that are widely expressed in neurons of many areas of the brain (Khakh and North, 2012) and neuroendocrine cells (Stojilkovic and Zemkova, 2013) might be involved in the adverse neuropsychiatric effects of anabolic steroids.

In conclusion, our data revealed that 17 β -ester derivatives of testosterone are effective positive P2X2R and P2X4R allosteric modulators that antagonize the effect of ivermectin on P2X4R channel deactivation, suggesting binding in the transmembrane domain. The obtained structure-activity relationship data revealed structural elements required by putative binding site(s) on P2XR for interactions with testosterone derivatives, and might be used in future for design of a topological model of action of testosterone derivatives and definition of pharmacophore.

Acknowledgements and conflict of interest disclosure

This work was supported by grants from the Grant Agency of the Czech Republic (16-12695S, 18-05413S and P208/12/G016), Charles University Grant Agency (928517) the Ministry of Education, Youth and Sports of the Czech Republic within the LQ1604 National Sustainability Program II (Project BIOCEV-FAR) and the project BIOCEV (CZ.1.05/1.1.00/02.0109), and by the Czech

Academy of Sciences research projects RVO 67985823, RVO 61388963. The authors of this publication have no conflict of interest to declare. All experiments were conducted in compliance with the ARRIVE guidelines.

All experiments were conducted in compliance with the ARRIVE guidelines.

Open science badges

This article has received a badge for *Open Materials* because it provided all relevant information to reproduce the study in the manuscript. The complete Open Science Disclosure form for this article can be found at the end of the article. More information about the Open Practices badges can be found at <https://cos.io/our-services/open-science-badges/>.

Supporting information

Additional supporting information may be found online in the Supporting Information section at the end of the article.

Scheme S1. Synthesis of compounds 4–6, 10 and 12–16.^a

Appendix S1. Supplementary Materials and methods.

Figure S1. Lack of effect of testosterone butyrate on deactivation properties of P2X7R.

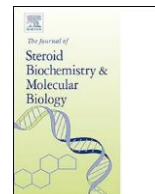
Table S1. Summary of computational values of physicochemical properties of compounds 1–16.

Table S2. Concentration-dependent effects of testosterone and testosterone derivatives on P2X4R currents.

References

- Ahrens J., Leuwer M., Demir R., Krampfl K., Foadi N. and Haeseler G. (2008) The anaesthetic steroid alphaxalone positively modulates alpha1-glycine receptor function. *Pharmacology* 82, 228–232.
- Ase A. R., Honson N. S., Zaghdane H., Pfeifer T. A. and Seguela P. (2015) Identification and characterization of a selective allosteric antagonist of human P2X4 receptor channels. *Mol. Pharmacol.* 87, 606–616.
- Baulieu E. E. (1998) Neurosteroids: a novel function of the brain. *Psychoneuroendocrinology* 23, 963–987.
- Burnstock G. (2006) Purinergic signalling—an overview. *Novartis Found. Symp.* 276, 26–48; discussion 48–57, 275–281.
- Coddou C., Stojilkovic S. S. and Huidobro-Toro J. P. (2011) Allosteric modulation of ATP-gated P2X receptor channels. *Rev. Neurosci.* 22, 335–354.
- Codocedo J. F., Rodriguez F. E. and Huidobro-Toro J. P. (2009) Neurosteroids differentially modulate P2X ATP-gated channels through non-genomic interactions. *J. Neurochem.* 110, 734–744.
- Collo G., Neidhart S., Kawashima E., Kosco-Vilbois M., North R. A. and Buell G. (1997) Tissue distribution of the P2X7 receptor. *Neuropharmacology* 36, 1277–1283.
- Evans R. J. (2009) Orthosteric and allosteric binding sites of P2X receptors. *Eur. Biophys. J.* 38, 319–327.
- Ganesan K. and Pellegrini M. V. (2018) *Anabolic Steroids*. StatPearls, Treasure Island, FL.
- Harrison N. L. and Simmonds M. A. (1984) Modulation of the GABA receptor complex by a steroid anaesthetic. *Brain Res.* 323, 287–292.

- Hattori M. and Gouaux E. (2012) Molecular mechanism of ATP binding and ion channel activation in P2X receptors. *Nature* 485, 207–212.
- Hojo Y. and Kawato S. (2018) Neurosteroids in adult hippocampus of male and female rodents: biosynthesis and actions of sex steroids. *Front. Endocrinol.* 9, 183.
- Hosie A. M., Wilkins M. E., da Silva H. M. and Smart T. G. (2006) Endogenous neurosteroids regulate GABAA receptors through two discrete transmembrane sites. *Nature* 444, 486–489.
- Huang X., Chen H. and Shaffer P. L. (2017) Crystal structures of human GlyR α 3 bound to ivermectin. *Structure* 25, e942.
- Inoue K., Tsuda M. and Koizumi S. (2004) ATP- and adenosine-mediated signaling in the central nervous system: chronic pain and microglia: involvement of the ATP receptor P2X4. *J. Pharmacol. Sci.* 94, 112–114.
- Jelinkova I., Yan Z., Liang Z., Moonat S., Teisinger J., Stojilkovic S. S. and Zemkova H. (2006) Identification of P2X(4) receptor-specific residues contributing to the ivermectin effects on channel deactivation. *Biochem. Biophys. Res. Commun.* 349, 619–625.
- Karasawa A., Michalski K., Mikhelzon P. and Kawate T. (2017) The P2X7 receptor forms a dye-permeable pore independent of its intracellular domain but dependent on membrane lipid composition. *eLife* 6, e31186.
- Khakh B. S. and North R. A. (2012) Neuromodulation by extracellular ATP and P2X receptors in the CNS. *Neuron* 76, 51–69.
- Khakh B. S., Proctor W. R., Dunwiddie T. V., Labarca C. and Lester H. A. (1999) Allosteric control of gating and kinetics at P2X(4) receptor channels. *J. Neurosci.* 19, 7289–7299.
- Latapiat V., Rodriguez F. E., Godoy F., Montenegro F. A., Barrera N. P. and Huidobro-Toro J. P. (2017) P2X4 receptor in silico and electrophysiological approaches reveal insights of ivermectin and zinc allosteric modulation. *Front. Pharmacol.* 8, 918.
- Lorca R. A., Rozas C., Loyola S., Moreira-Ramos S., Zeise M. L., Kirkwood A., Huidobro-Toro J. P. and Morales B. (2011) Zinc enhances long-term potentiation through P2X receptor modulation in the hippocampal CA1 region. *Eur. J. Neurosci.* 33, 1175–1185.
- Lynagh T. and Lynch J. W. (2012) Molecular mechanisms of Cys-loop ion channel receptor modulation by ivermectin. *Front. Mol. Neurosci.* 5, 60.
- Mackay L., Zemkova H., Stojilkovic S. S., Sherman A. and Khadra A. (2017) Deciphering the regulation of P2X4 receptor channel gating by ivermectin using Markov models. *PLoS Comput. Biol.* 13, e1005643.
- Monif M., Reid C. A., Powell K. L., Smart M. L. and Williams D. A. (2009) The P2X7 receptor drives microglial activation and proliferation: a trophic role for P2X7R pore. *J. Neurosci.* 29, 3781–3791.
- Muller C. E. (2015) Medicinal chemistry of P2X receptors: allosteric modulators. *Curr. Med. Chem.* 22, 929–941.
- Munetsuna E., Hojo Y., Hattori M., Ishii H., Kawato S., Ishida A., Kominami S. A. and Yamazaki T. (2009) Retinoic acid stimulates 17 β -estradiol and testosterone synthesis in rat hippocampal slice cultures. *Endocrinology* 150, 4260–4269.
- Murrell-Lagnado R. D. (2017) Regulation of P2X purinergic receptor signaling by cholesterol. *Curr. Top. Membr.* 80, 211–232.
- Nicke A., Baumert H. G., Rettinger J., Eichele A., Lambrecht G., Mutschler E. and Schmalzing G. (1998) P2X1 and P2X3 receptors form stable trimers: a novel structural motif of ligand-gated ion channels. *EMBO J.* 17, 3016–3028.
- North R. A. (2002) Molecular physiology of P2X receptors. *Physiol. Rev.* 82, 1013–1067.
- Paradiso K., Zhang J. and Steinbach J. H. (2001) The C terminus of the human nicotinic α 4 β 2 receptor forms a binding site required for potentiation by an estrogenic steroid. *J. Neurosci.* 21, 6561–6568.
- Priel A. and Silberberg S. D. (2004) Mechanism of ivermectin facilitation of human P2X4 receptor channels. *J. Gen. Physiol.* 123, 281–293.
- De Roo M., Rodeau J. L. and Schlichter R. (2003) Dehydroepiandrosterone potentiates native ionotropic ATP receptors containing the P2X2 subunit in rat sensory neurones. *J. Physiol.* 552, 59–71.
- Rupprecht R. and Holsboer F. (1999) Neuroactive steroids: mechanisms of action and neuropsychopharmacological perspectives. *Trends in Neurosciences.* 22(9), 410–416.
- Sedlacek M., Korinek M., Petrovic M., Cais O., Adamusova E., Chodounska H. and Vyklicky L., Jr (2008) Neurosteroid modulation of ionotropic glutamate receptors and excitatory synaptic transmission. *Physiol. Res.* 57(Suppl 3), S49–57.
- Soto F., Garcia-Guzman M., Gomez-Hernandez J. M., Hollmann M., Karschin C. and Stuhmer W. (1996) P2X4: an ATP-activated ionotropic receptor cloned from rat brain. *Proc. Natl Acad. Sci. USA* 93, 3684–3688.
- Stojilkovic S. S. and Zemkova H. (2013) P2X receptor channels in endocrine glands. *Wiley Interdiscip. Rev. Membr. Transp. Signal.* 2, 173–180.
- Vavra V., Bhattacharya A. and Zemkova H. (2011) Facilitation of glutamate and GABA release by P2X receptor activation in supraoptic neurons from freshly isolated rat brain slices. *Neuroscience* 188, 1–12.
- Virginio C., MacKenzie A., Rassendren F. A., North R. A. and Surprenant A. (1999) Pore dilation of neuronal P2X receptor channels. *Nat. Neurosci.* 2, 315–321.
- Xu H., Wu B., Jiang F., et al (2013) High fatty acids modulate P2X(7) expression and IL-6 release via the p38 MAPK pathway in PC12 cells. *Brain Res. Bull.* 94, 63–70.
- Yan Z., Khadra A., Sherman A. and Stojilkovic S. S. (2011) Calcium-dependent block of P2X7 receptor channel function is allosteric. *J. Gen. Physiol.* 138, 437–452.
- Zemkova H. and Vanecek J. (2000) Differences in gonadotropin-releasing hormone-induced calcium signaling between melatonin-insensitive and melatonin-insensitive neonatal rat gonadotrophs. *Endocrinology* 141, 1017–1026.
- Zemkova H., Balik A., Jiang Y., Kretschmannova K. and Stojilkovic S. S. (2006) Roles of purinergic P2X receptors as pacemaking channels and modulators of calcium-mobilizing pathway in pituitary gonadotrophs. *Mol. Endocrinol.* 20, 1423–1436.
- Zemkova H. W., Bjelobaba I., Tomic M., Zemkova H. and Stojilkovic S. S. (2008) Molecular, pharmacological and functional properties of GABA(A) receptors in anterior pituitary cells. *J. Physiol.* 586, 3097–3111.
- Zemkova H., Kucka M., Li S., Gonzalez-Iglesias A. E., Tomic M. and Stojilkovic S. S. (2010) Characterization of purinergic P2X4 receptor channels expressed in anterior pituitary cells. *Am. J. Physiol. Endocrinol. Metab.* 298, E644–651.
- Zemkova H., Tvrdonova V., Bhattacharya A. and Jindrichova M. (2014) Allosteric modulation of ligand gated ion channels by ivermectin. *Physiol. Res.* 63(Suppl 1), S215–224.
- Zemkova H., Khadra A., Rokic M. B., Tvrdonova V., Sherman A. and Stojilkovic S. S. (2015) Allosteric regulation of the P2X4 receptor channel pore dilation. *Pflugers Arch.* 467, 713–726.



Lithocholic acid inhibits P2X2 and potentiates P2X4 receptor channel gating

Sonja Sivceva^{a,b}, Barbora Slavikova^c, Milorad Ivetic^{a,b}, Michal Knezu^{a,b}, Eva Kudova^c, Hana Zemkova^{a,*}

^a Institute of Physiology, Czech Academy of Sciences, Prague, Czech Republic

^b Faculty of Science, Charles University, Prague, Czech Republic

^c Institute of Organic Chemistry and Biochemistry, Czech Academy of Sciences, Prague, Czech Republic

ARTICLE INFO

Keywords:

ATP
Purinergic P2X receptors
Bile acids
Lithocholic acid
Ivermectin
Allosteric modulation

ABSTRACT

The family of ATP-gated purinergic P2X receptors comprises seven bunits (P2X1-7) that are unevenly distributed in the central and peripheral nervous systems as well as other organs. Endogenous modulators of P2X receptors are phospholipids, steroids and neurosteroids. Here, we analyzed whether bile acids, which are natural products derived from cholesterol, affect P2X receptor activity. We examined the effects of primary and secondary bile acids and newly synthesized derivatives of lithocholic acid on agonist-induced responses in HEK293T cells expressing rat P2X2, P2X4 and P2X7 receptors. Electrophysiology revealed that low micromolar concentrations of lithocholic acid and its structural analog 4-dafachronic acid strongly inhibit ATP-stimulated P2X2 but potentiate P2X4 responses, whereas primary bile acids and other secondary bile acids exhibit no or reduced effects only at higher concentrations. Agonist-stimulated P2X7 responses are significantly potentiated by lithocholic acid at moderate concentrations. Structural modifications of lithocholic acid at positions C-3, C-5 or C-17 abolish both inhibitory and potentiation effects to varying degrees, and the 3 α -hydroxy group contributes to the ability of the molecule to switch between potentiation and inhibition. Lithocholic acid allosterically modulates P2X2 and P2X4 receptor sensitivity to ATP, reduces the rate of P2X4 receptor desensitization and antagonizes the effect of ivermectin on P2X4 receptor deactivation. Alanine-scanning mutagenesis of the upper half of P2X4 transmembrane domain-1 revealed that residues Phe48, Val43 and Tyr42 are important for potentiating effect of lithocholic acid, indicating that modulatory sites for lithocholic acid and ivermectin partly overlap. Lithocholic acid also inhibits ATP-evoked currents in pituitary gonadotrophs expressing native P2X2, and potentiates ATP currents in unidentified pituitary cells expressing P2X4 receptors. These results indicate that lithocholic acid is a bioactive steroid that may help to further unveil the importance of the P2X2, and P2X4 receptors in many physiological processes.

1. Introduction

Purinergic P2X receptors are ATP-gated cation channels that are expressed in various tissues and have multiple roles in the central and peripheral nervous systems, immune system, endocrine system, as well as in other organs [1]. The family of P2X receptors comprises seven subunits (P2X1-7) that assemble as homo- or heterotrimers [2]. Each P2X receptor subunit consists of a large extracellular ATP-binding domain, two transmembrane domains and intracellular N- and C-termini [3–7]. Crystal structures of the zebrafish P2X4 receptor have fully confirmed the trimeric structure of the functional P2X receptor, the helical organization of the transmembrane domain and have revealed

the intersubunit location of an orthosteric ATP binding site [8,9].

The activity of P2X receptors might be regulated by several endogenous and exogenous compounds acting as allosteric modulators that enhance or block receptor function [10–13]. Endogenous allosteric modulators include calcium ions [14], essential trace metals [11], free fatty acids [15] and neurosteroids [16–18] synthesized in the central and peripheral nervous systems from cholesterol, or imported from peripheral sources [19,20]. Neurosteroids have been reported to positively modulate [16–18] or negatively modulate [17] P2X2 and P2X4 receptor function. P2X7 function is modulated by cholesterol and other membrane lipids through direct interactions with the transmembrane domain [21–23]. Little is known about the modulation of P2X receptors

Abbreviations: (BzATP), 2'3'-O-(Benzoyl-4-benzoyl)-ATP; (EC₅₀), a concentration producing 50 % of the maximal response; (IC₅₀), a concentration producing 50 % of the maximal inhibition; (GABA), γ -aminobutyric acid; (HEK), human embryonic kidney

* Corresponding author at: Institute of Physiology, Czech Academy of Sciences, Videnska 1083, 142 20, Prague 4, Czech Republic.

E-mail address: zemkova@biomed.cas.cz (H. Zemkova).

<https://doi.org/10.1016/j.jsmb.2020.105725>

Received 27 February 2020; Received in revised form 21 June 2020; Accepted 5 July 2020

Available online 8 July 2020

0966-1839/© 2020 Elsevier Ltd. All rights reserved.

by bile acids, other natural circulating products of cholesterol, which are considered to modulate other cell surface receptors and ion channels [24,25].

Bile acids are synthesized from cholesterol by hepatocytes in the liver. Primary bile acids (cholic acid and chenodeoxycholic acid) are partially converted into secondary bile acids (deoxycholic acid, lithocholic acid and ursodeoxycholic acid) by dehydroxylation, which increases the hydrophobicity of the molecule and therefore their accumulation in the plasma membrane [26]. In humans, the most abundant secondary bile acids are lithocholic acid and deoxycholic acid [27]. Endogenous lithocholic acid has been reported to dilate cerebral arteries via activation of the Ca^{2+} /voltage-gated K^{+} large conductance (BK) channel [24,28,29], and deoxycholic acid is a potent antagonist at N-methyl-D-aspartic acid (NMDA) and GABA(A) receptors in hypothalamic neurons [30]. Recently, it has been reported that the rat P2X2 receptor, but not other P2X receptor subtypes, is inhibited by several bile acids, particularly lithocholic acid and hyodeoxycholic acid [31], whereas another study reported that deoxycholic acid strongly inhibits the human P2X4 receptor [32]. Despite these two studies in the literature aiming to describe the effects of bile acids on P2X receptors, their role is still controversial.

Here, we tested a hypothesis that bile acids modulate rat P2X2, P2X4 and P2X7 receptors. We designed and synthesized new derivatives of lithocholic acid and analyzed their mechanism of action. The results show that lithocholic acid and its derivative 4-dafachronic acid inhibit P2X2 but potentiate P2X4 receptors at low micromolar concentrations, while P2X7 receptor is only slightly potentiated; other primary and secondary bile acids produce no or reduced effects only at higher doses.

2. Materials and methods

2.1. Cell culture and transfection

Experiments were performed using HEK293T cell line (ATCC® CRL3216™, Manassas, VA, USA). Cells were grown in Dulbecco's modified Eagle's medium, DMEM (Gibco, Cat. #41966-029, Rockville, MD, USA) supplemented with 10 % fetal bovine serum (ATCC, Cat. #302021, Manassas, VA, USA) 50 U/mL penicillin and 50 µg/mL streptomycin (SIGMA, Cat. #A5955, St Louis, MO, USA) in a humidified 5 % CO_2 atmosphere at 37 °C. Passaging was performed for 1–2 months, maximum number of passages was 20. The cells were cultured in 75 cm^2 plastic culture flasks (Nunc, Cat. #156367, Rochester, NY, USA) for 36–72 h until they reached 80–95 % confluence. On the day before transfection, ~150,000 cells were seeded on 35 mm culture dishes (Sarstedt, Newton, NC, USA) and incubated at 37 °C for at least 24 h. Transfection was performed using 2 µg of DNA and 2 µl of jetPRIME™ reagent (PolyPlus, Cat. #114–15) in 2 mL of Dulbecco's modified Eagle's medium according to the manufacturer's instructions (PolyPlus-transfection, Illkirch, France). After 24 h of incubation, the transfected cells were mechanically dispersed and re-seeded on 35 mm culture dishes (Corning, Cat. #3294, NY, USA) for 2–6 hours prior to recording.

2.2. DNA constructs

Rat full-length P2X2, P2X4 and P2X7 cDNA subcloned into the bicistronic enhanced fluorescent protein expression vector, pIRES2-EGFP (Clontech, Mountain View, CA, USA; RRID:Addgene_43964) was a gift from Dr. S.S. Stojilkovic, NICHD/NIH, Bethesda, USA. The rat P2X4-pIRES2-EGFP construct was used for generation of alanine mutants [33,34]. Oligonucleotides (synthesized by VBC-Genomics, Vienna, Austria and Sigma Chemical Company, USA) containing specific point mutations were introduced into the rP2X4-pIRES2-EGFP template using Pfu Ultra DNA polymerase (Fermentas International Inc, USA). A High-Speed Plasmid Mini Kit (Geneaid, Shijr City, Taipei County, Taiwan) was used to isolate plasmids for transfection. Dye terminator cycle

sequencing (ABI PRISM3100, Applied Biosystems, Foster City, CA) was used to identify and verify the presence of the mutations

2.3. Patch clamp recordings

Currents were recorded in a whole-cell configuration using an Axopatch 200B patch-clamp amplifier (Axon Instruments, Union City, CA, USA) and stored using the pClamp 9.0 software package in conjunction with the Digidata 1322A A/D converter (Molecular Devices, Silicon Valley, CA, USA). Patch electrodes were pulled from borosilicate glass capillaries with firepolished ends, OD = 1.50 mm, ID = 0.86 mm, Length = 8 cm (type GB150F-8 P; Science Products GmbH, Hofheim, Germany) using a Flaming Brown horizontal puller (P-87; Sutter Instruments, Novato, CA), and heat-polished to a final tip resistance of 3–5 10 MΩ. The experiments were performed on single cells with an average capacitance of 10 pF, and the membrane potential was held at –60 mV. The access resistance (average 13.8 ± 2.2 MΩ) was monitored throughout each experiment. Whole-cell recording was performed with 70–80 % series resistance compensation. Only cells with steady state leak current lower than 200 pA were used in subsequent analysis. Patch electrodes were filled with a solution containing 154 mM CsCl, 11 mM EGTA 11, and 10 mM HEPES; the pH was adjusted to 7.2 using 1 M CsOH. The osmolarity of intracellular solution was 293 mOsm. During the experiments, cells were continuously perfused with an extracellular solution containing 142 mM NaCl, 3 mM KCl, 2 mM CaCl_2 , 1 mM MgCl_2 , 10 mM HEPES and 10 mM D-glucose and adjusted to pH 7.3 using 1 M NaOH. The stock solutions of 20 mM steroids in dimethyl sulfoxide were prepared from fresh powder stock every 6 months, and stored at –20 °C. Solutions containing ATP and steroids were applied using the RSC-200 Rapid Solution Changer (Biologic, Claix, France).

2.4. Animals, brain slices and pituitary cultures

All animal procedures were approved by the Animal Care and Use Committee of the Czech Academy of Sciences (dissection protocol # 67,985,823). Wistar rats (RRID:RGD_13508588) were obtained from Animal Facility of the Institute of Physiology, Czech Academy of Sciences, approved by Ministry of Environment to use (approval number #56,379/2015-MZE-17,214), and breed and distribute (approval number #1398/2014-MZE-17,214) animals. Breeding pairs of rats were used to produce male and female rats for brain slices and anterior pituitary cell preparations. Rats were housed in cages (42 × 26 × 22 cm; 1–2 rats per cage) with wood shavings bedding (LIGNOCEL® 3–4 S; JRS, Rosenberg, Germany), and provided with breeding diet for rats (Altromin, Cat. #1314, Velaz, Prague, Czech Republic) and fresh water at libitum. Cages were kept in ventilated racks in an acclimated room (at 22 ± 2 °C, with 55 % humidity), and lights on from 6 AM to 6 PM. Brains or pituitary glands were removed between 11 AM and 6 PM. Six adult rats were used for brain slices preparations, and 3–6 newborn rats for anterior pituitary cell preparation; in total 3 pituitary cell culture preparations were performed. Animals of both sexes were used in this study. Euthanasia was performed by decapitation after anaesthesia with isofurane (Forane, Cat. #B506, AbbVie, Prague Czech Republic).

Brain slices containing the supraoptic nucleus (SON) were prepared from 16- to 24-day-old rats (30–35 g weight) as described previously [35]. Briefly, brains were removed after decapitation and placed in ice-cold (4 °C) oxygenated (95 % O_2 + 5% CO_2) artificial cerebrospinal fluid (ACSF). Hypothalamic slices (200- to 300-µm-thick) were cut with a vibratome (DTK-1000, D.S.K. Dosaka, Japan). Slices were pre-incubated for at least 1 h at 32–33 °C in oxygenated ACSF that contained the following components: 130 mM NaCl, 3 mM KCl, 1 mM MgCl_2 , 2 mM CaCl_2 , 19 mM NaHCO_3 , 1.25 mM NaH_2PO_4 , and 10 mM glucose (pH 7.3–7.4; osmolality 300–315 mOsm). During the experiments, slices in recording chamber were submerged in continuously flowing oxygenated ACSF at a rate of 1–2 mL min^{-1} at room

temperature. Drugs were diluted and applied for 10–20 s in a HEPES-buffered extracellular solution that was used for no more than 2 min. Slices were viewed with an upright microscope (Olympus BX50WI, Melville, NY, USA) mounted on a Gibraltar X-Y table (Burleigh) using a water immersion lens (60x and 10x) and Dodt infrared gradient contrast (Luigs & Neumann, GmbH, Germany). SON were identified by the position relative to the chiasma opticum [35].

Pituitary cells from 4 to 7 day-old rats (8–10 g weight) were dispersed as described previously [36]. Briefly, animals were decapitated without anaesthesia, anterior pituitaries were extracted and washed in medium 199 (GIBCO, Cat. #22340–020) containing sodium bicarbonate, 10 % heat-inactivated fetal bovine serum (Sigma, Cat. #F9665), penicillin (100 U/mL) and streptomycin (100 µg/mL) (GIBCO, Cat. #15140–122), 2 mM glutamine, and treated with papain (Worthington biochemical, Cat. #LS003119) for 15 min at 37 °C. The cells were mechanically dispersed using a glass pipette (BRAND GmbH, Cat. # 1780.0150), harvested by centrifugation at 300 g for 10 min, and the resulting cell pellet was resuspended in medium 199 and cultured in an air/CO₂ atmosphere at 37 °C. For electrophysiology, 0.1–0.2 million cells (in a 200-µL drop) were plated onto 25-mm glass coverslips coated with 1% poly-L-lysine and cultured in a humidified 5% CO₂ atmosphere at 37 °C. Experiments were performed 24–72 h after dispersion.

Patch electrodes used for whole-cell recording from neurons and pituitary cells were filled with an intracellular solution containing: 140 mM KCl, 3 mM MgCl₂, 0.5 mM CaCl₂, 10 mM HEPES, and 5 mM EGTA, pH adjusted to 7.2 with KOH. In current-clamp mode, only cells with resting membrane potential more negative than –40 mV were examined.

2.5. Calculations

The concentration-response data points were fitted with the equation $y = I_{max}/[1 + (EC_{50}/x)^h]$, where y is the amplitude of the current evoked by ATP, I_{max} is the maximum current amplitude induced by 100 µM ATP, EC_{50} is the agonist concentration producing 50 % of the maximal response, h is the Hill coefficient, and x is the concentration of ATP (SigmaPlot 2000 v9.01; SPSS Inc., Chicago, IL; RRID:SCR_003210). The kinetics of desensitization or deactivation (current decay evoked by washout of agonists) were fitted by a single exponential function ($y = A_1 \exp(-t/\tau)$) or by the sum of two exponentials ($y = A_1 \exp(-t/\tau_1) + A_2 \exp(-t/\tau_2)$) using the program pClamp 10 (Molecular Devices), where A_1 and A_2 are relative amplitudes of the first and second exponentials, and τ_1 and τ_2 are the time constants. The derived time constants for deactivation and desensitization were labeled as τ_{off} and τ_{des} , respectively. Weight desensitization constant was calculated as $y = [(A_1\tau_{des1}) + (A_2\tau_{des2})]/(A_1 + A_2)$.

2.6. Statistical analysis

All numerical values in the text are reported as the mean \pm SEM. Comparisons between two groups were performed by Student's unpaired t -test (** $p < 0.01$ and * $p < 0.05$). Statistical comparison of multiple groups was made by using one-way ANOVA followed by Tukey's post-hoc test in SigmaStat 2000 v9.0, for comparison to a single control. In the case of pituitary cells or SON neurons when ATP-induced responses were recorded from the same cell in the presence and absence of steroid, Student's paired t -test was used. The "n" indicates number of cells throughout the study, if not otherwise stated.

2.7. Chemicals and synthesis of new lithocholic acid derivatives

We first examined common primary and secondary bile acids (Fig. 1A): 3 α ,7 α ,12 α -trihydroxy-5 β -cholanolic acid (Cholic acid, Compound 1), 3 α ,7 α -dihydroxy-5 β -cholanolic acid (Chenodeoxycholic acid, Compound 2), 3 α ,12 α -dihydroxy-5 β -cholanolic acid (Deoxycholic acid, Compound 3), 3 α ,7 β -dihydroxy-5 β -cholanolic acid (Ursodeoxycholic

acid, Compound 4) and 3 α -hydroxy-5 β -cholanolic acid (Lithocholic acid, Compound 5) that were purchased from SIGMA (St. Louis, MO). Then we designed and synthesized new derivatives of lithocholic acid (Supplementary information and Fig. 1B) in order to increase its modulatory effects: 3 β -Hydroxy-5 β -cholanolic acid (Isolithocholic acid, Compound 6), 3-Oxo-5 β -cholanolic acid (Compound 7), 5 β -Cholanolic acid-3 α -yl acetate (Compound 8), 3 α -Hydroxy-5 α -cholanolic acid (Compound 9), 3 β -Hydroxy-5 α -cholenolic acid (Compound 12), 3 α -Hydroxy-5 β -cholanolic acid methyl ester (Compound 13) and N-(3 α -Hydroxy-5 β -cholan-24-oyl)-glycine (Compound 14). 3 β -Hydroxy-5 α -cholanolic acid (CAS 2276–93-9, Compound 10) was purchased from Alfa Chemistry, 1360 Stony Brook Rd, Stony Brook, NY 11790, USA, (Cat. #ACM2276939), 4-Dafachronic acid (CAS 23017–97-2, Compound 11) was purchased from DIVERCHIM SA, Damjanich utca, Budapest, 1071, Hungary, (Cat. #CAYM14100), 12-Oxo-5 β -cholanolic acid (CAS 63042–31-9, Compound 15) was purchased from Chemieliva Pharmaceutical (Cat. #CE054077) and obeticholic acid (CAS 459789–99-2, Compound 16) was purchased from MCE® MedChemExpress (Cat. #HY-12,222). All newly synthesized compounds have been prepared from lithocholic acid (Supplementary information). Ivermectin (Cat. #18898) and all other chemicals were from SIGMA (St. Louis, MO).

3. Results

3.1. Testing of primary and secondary bile acids and identification of lithocholic acid as the most potent inhibitor of P2X2 and activator of P2X4 receptor function

The abilities of five common primary and secondary bile acids (compounds 1–5, Fig. 1A) to modulate P2X receptor function were examined using patch clamp whole-cell recordings in HEK293T cells expressing rat P2X2, P2X4 and P2X7 receptors. We measured the amplitude of P2X2 and P2X4 current induced by a short (2–5 s) application of 1 µM ATP (applied every 20 s) in the presence and absence of 3 µM bile acid. Repetitive stimulation of P2X4 receptor produces rundown of responses that is due to receptor desensitization, responsiveness to ATP and receptor number [37]. The effect of bile acids on this receptor was thus tested as a ratio of maximum current amplitude in the presence of drug and mean amplitude of currents before its application and after washout. Electrophysiology revealed that cholic acid (Fig. 2A), chenodeoxycholic acid (Fig. 2B), deoxycholic acid (Fig. 2C) and ursodeoxycholic acid (Fig. 2D) exhibited no effects. Lithocholic acid (Fig. 2E) significantly inhibited P2X2 (59 ± 2.3 %, $n = 60$, $P < 0.01$) and potentiated P2X4 responses (179 ± 6.6 %, $n=59$, $P < 0.01$) without significantly affecting P2X7 responses (116 ± 3.8 %, $n=19$, $P > 0.05$; Fig. 2F, upper trace) stimulated with 15 µM BzATP, an artificial but potent agonist of the P2X7 receptor [1].

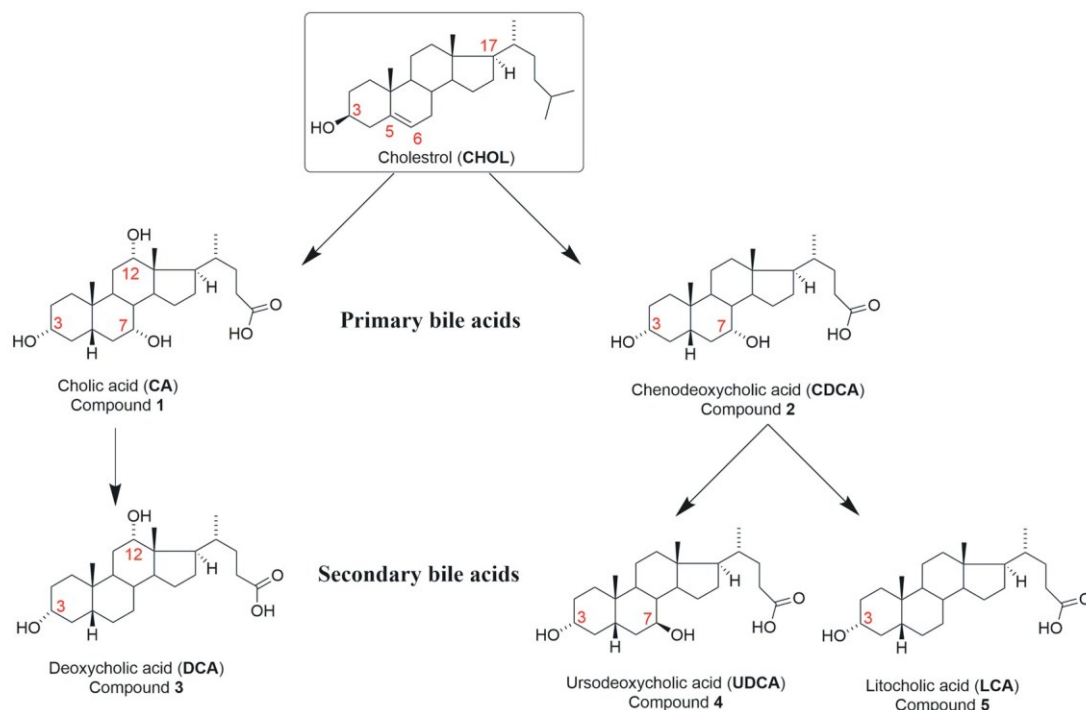
Lithocholic acid (10 µM) produced a maximal effect on ATP-evoked current amplitude within 40 s of application with a time constant (τ_{ON}) of about 20 s (P2X2: $\tau_{ON} = 18.9 \pm 6.1$ s, $n = 3$; P2X4: $\tau_{ON} = 24.3 \pm 2.3$ s, $n = 7$; Fig. S1). The effect was fully reversible within 3 min of washing with a time constant (τ_{OFF}) of about 30 s (P2X2: $\tau_{OFF} = 25.8 \pm 7.9$ s, $n = 3$; P2X4: $\tau_{OFF} = 35.3 \pm 5.8$ s, $n = 7$; Fig. S1).

These results showed that lithocholic acid is an effective negative modulator of P2X2 and a positive modulator of the P2X4 receptor and that primary bile acids or other secondary bile acids exhibit no significant effect at low micromolar concentrations.

3.2. Concentration-dependent effects of bile acids and structural analogues of lithocholic acid

We measured the amplitude of 1 µM ATP-induced P2X2 or P2X4 currents in the presence of various concentrations (1, 3, 10 or 30 µM) of primary and secondary bile acids (Fig. 1A) and lithocholic acid derivatives (Fig. 1B) to further characterize the bile acid-induced modulatory effects; concentrations greater than 30 µM were not tested due

A



B

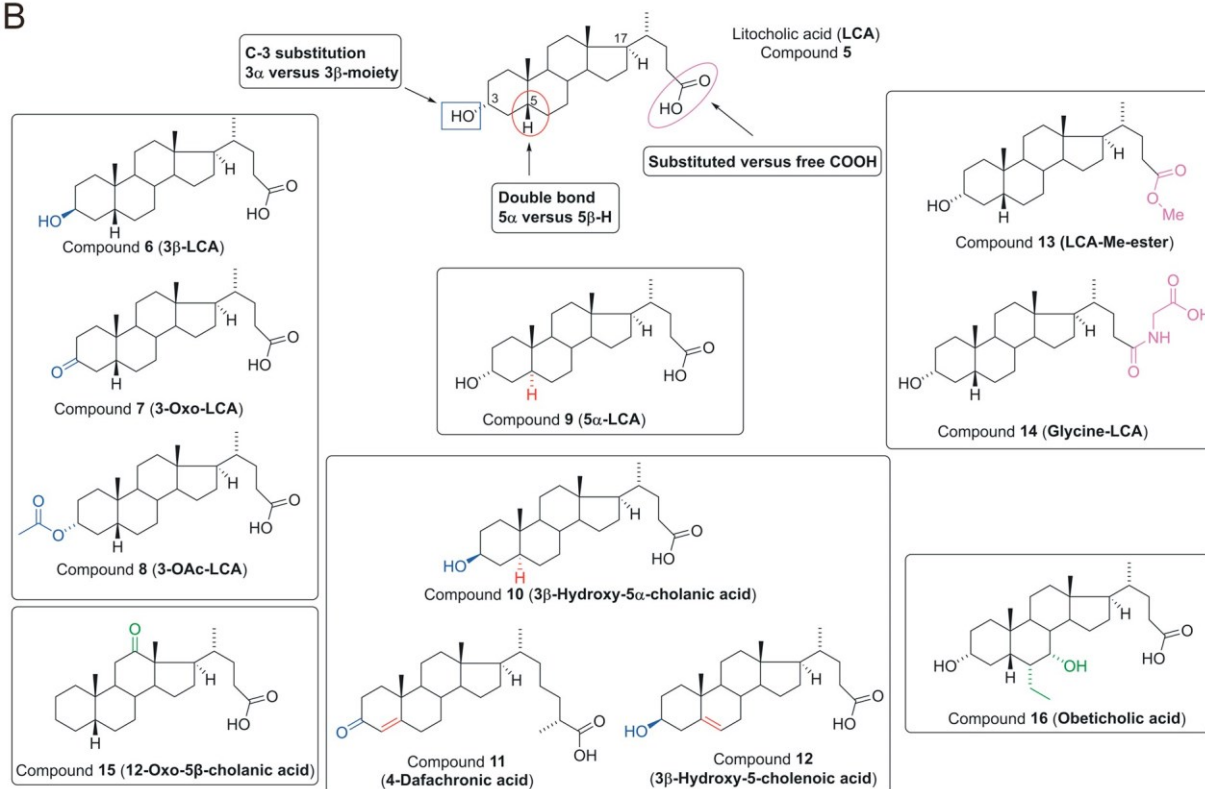


Fig. 1. Bile acids and their analogues studied in this work. (A) Primary and secondary bile acids (compounds 1 – 5) that are endogenously synthesized from cholesterol. (B) Structural analogues of lithocholic acid that were newly synthesized in our laboratory (compounds 6 – 9 and 12 – 14; see Supplementary Information) or purchased from commercial sources (compounds 10, 11, 15 and 16). Three types of modifications of lithocholic acid were tested in this study: modifications at positions C-3, C-5 and C-17 (see also Supplementary Information).

to the poor solubility of some compounds at these concentrations. We used commercially available structural analogues of lithocholic acid (compounds 10, 11, 15 and 16), as well as newly synthesized

derivatives (compounds 6, 7, 8, 9, 12, 13 and 14) that were designed in order to increase the lithocholic acid-induced modulatory effects and/or to identify critical structural features of this molecule. Lithocholic

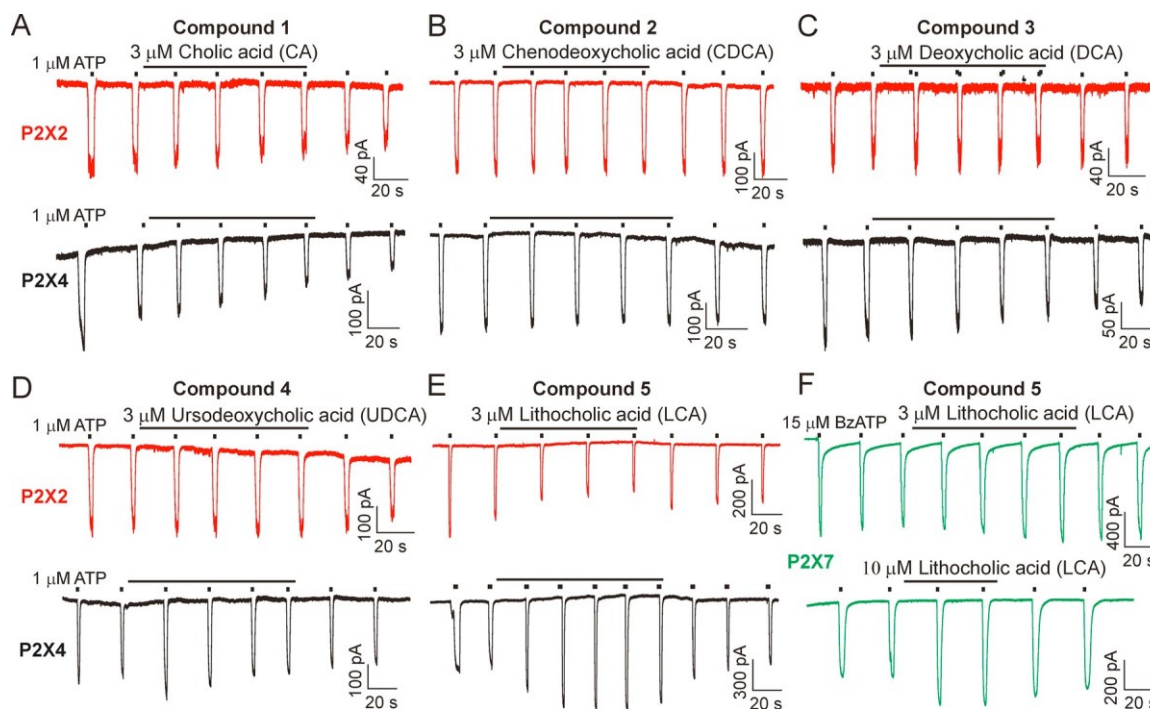


Fig. 2. Effect of primary and secondary bile acids on agonist-induced currents in HEK293T cells expressing rat P2X2, P2X4 and P2X7 receptors. (A - E) Example recordings from cells expressing the rat P2X2 receptor (red traces) or P2X4 receptor (black traces) and stimulated with 1 μ M ATP (2-s pulse applied every 20 s) in the presence or absence of bile acids: cholic acid (A), chenodeoxycholic acid (B), deoxycholic acid (C), ursodeoxycholic acid (D) and lithocholic acid (E); all at 3 μ M. (F) Example recordings from cells transfected with the rat P2X7 receptor showing the effect of 3 μ M lithocholic acid (upper trace) and 10 μ M lithocholic acid (lower trace) on responses stimulated by application of 15 μ M BzATP. In this and other figures, thin bars above the traces indicate bile acid application, and thick bars indicate agonist application.

acid was modified at positions C-3 (compounds **6-8**) and C-5 (compounds **9-12**) and by esterification or conjugation with glycine (compounds **13** and **14**). The results of these investigations are summarized in [Table 1](#).

Lithocholic acid inhibited P2X2 and potentiated P2X4 receptors in a concentration-dependent manner ([Fig. 3A, B and E](#)), maximum effect was observed at 30 μ M (P2X2: 31 ± 11 %, $n = 5$, $P < 0.01$; P2X4: 391 ± 33 %, $n=12$, $P < 0.01$). Primary bile acids and other secondary bile acids exhibited a tendency to inhibit P2X2 and potentiate P2X4 receptors only at higher concentrations ([Fig. 3D](#)).

Structural change of the 3 α -OH to 3 β -OH (compound **6**; isolithocholic acid) or to 3-ketone (compound **7**) resulted in a significantly reduced potentiating effect on P2X4 (30 μ M compound **6**: 142 ± 7.2 %, $n = 5$, $P < 0.05$; 30 μ M compound **7**: 176 ± 23 %, $n = 12$, $P < 0.05$; [Fig. 3E](#)), while the inhibitory effect on P2X2 was well preserved (30 μ M compound **6**: 42 ± 5.2 %, $n = 5$, $P < 0.01$; 30 μ M compound **7**: 53 ± 12 %, $n = 12$, $P < 0.01$; [Fig. 3E](#)). An acetate moiety at position 3 α (compound **8**) completely abolished the inhibitory effect on the P2X2 receptor and equally potentiated both P2X2 and P2X4 receptors (30 μ M compound **8**, P2X2: 254 ± 22 %, $n = 5$, $P < 0.01$; P2X4: 243 ± 23 %, $n=12$, $P < 0.01$; [Fig. 3C and E](#)). The structural change of 5 β -H to 5 α -H (compounds **9** and **10**) or the double bond between C-5 and C-6 (compound **12**) completely abolished the potentiating effect on P2X4 and slightly reduced the inhibitory effect on P2X2 ([Fig. 3F](#)). The double bond between C-4 and C-5 (compound **11**, 4-dafachronic acid) had no effect on the inhibitory or potentiating activities (30 μ M P2X2: 53 ± 4.2 %, $n = 6$, $P < 0.01$; P2X4: 357 ± 84 %, $n=10$, $P < 0.01$), although no effect was observed at a concentration of 1 μ M ([Fig. 3F](#)). Esterification (compound **13**) completely abolished both the potentiating and inhibitory effects, and conjugation with glycine (compound **14**) partially reduced both effects ([Fig. 3G](#)). When applied at a higher doses (10–30 μ M), lithocholic acid significantly potentiated P2X7 responses (10 μ M LCA: 178 ± 15 %, $n = 10$, $P < 0.01$; 30 μ M

LCA: 259 ± 25 %, $n=9$, $P < 0.01$; [Fig. 2F](#), lower trace, and [Fig. 3G](#)), but this effect was not studied further.

In a concentration analysis on the P2X2 receptor, the concentration of lithocholic acid producing 50 % inhibition of the 1 μ M ATP-induced response (IC_{50}) was 4.6 ± 0.9 μ M ([Fig. 3H](#)).

To explain interesting properties of compound **8**, that is the only one from this series that bears hemiester moiety at C-3, we investigated compound **15** that also lacks the 3 α -hydroxy group, and thus the hydrogen that might form e.g. H-bond. Compound **15** (30 μ M) potentiated both P2X2 and P2X4 receptors similarly as compound **8** (P2X2: 211 ± 15 %, $n = 3$, $P < 0.01$; P2X4: 230 ± 53 %, $n=6$, $P < 0.01$; [Table 1](#)), indicating that 3 α -hydroxy group might be important for the ability of the molecule to switch between potentiation and inhibition.

We also evaluated the effect of obeticholic acid (compound **16**), the most active steroidal ligand for the farnesoid-X-receptor (FXR), bile acid receptor that might be endogenously expressed in HEK293 cells [[38](#)]. Obeticholic acid (3 μ M) had no effect on P2X2 or P2X4 responses, and slightly potentiated only P2X4 responses at higher doses (30 μ M; P2X2: 114 ± 11 %, $n = 3$, $P > 0.05$; P2X4: 182 ± 21 %, $n=4$, $P < 0.05$; [Table 1](#)), indicating that the effects of lithocholic acid are not due to modulation of P2X receptors via endogenous bile acid receptors.

These results showed that lithocholic acid and 4-dafachronic acid are robust inhibitors of the P2X2 receptor but activators of the P2X4 receptor, which are much more effective than the other principal bile acids or ligand for the FXR. Modifications of lithocholic acid at different parts of the steroid molecule did not identify a more potent analog but showed that all these modifications abolished both inhibitory and potentiating effects to varying degrees, and the C3 α -hydroxy group might

be important for the ability of the molecule to switch between potentiation and inhibition. However, a clear correlation between changes in the inhibitory effects on P2X2 and potentiating effects on P2X4 was not observed for the individual derivatives ([Fig. 3I](#)), suggesting that lithocholic acid might interact with P2X receptors at two modulatory

Table 1
Concentration-dependent effects of primary and secondary bile acids and lithocholic acid derivatives on P2X2 and P2X4 currents.

Compound	Receptor	1 μ M	3 μ M	10 μ M	30 μ M
1, CA	P2X2	n.d.	109 \pm 6.0	86 \pm 11	96 \pm 5.5
	P2X4	n.d.	109 \pm 3.4	123 \pm 3.0	129 \pm 16
2, CDCA	P2X2	n.d.	105 \pm 2.5	80 \pm 8.9	81 \pm 10
	P2X4	n.d.	108 \pm 2.4	119 \pm 6.2	132 \pm 14*
3, DCA	P2X2	n.d.	101 \pm 2.9	85 \pm 12	86 \pm 7
	P2X4	n.d.	118 \pm 9.5	119 \pm 4.0	144 \pm 22
4, UDCA	P2X2	n.d.	104 \pm 3.1	78 \pm 5.0*	75 \pm 6.1*
	P2X4	n.d.	113 \pm 2.8	127 \pm 8.3*	144 \pm 20
5, LCA	P2X2	76 \pm 6.9*	59 \pm 2.3**	39 \pm 5.5**	31 \pm 11**
	P2X4	159 \pm 7.0**	179 \pm 6.6**	249 \pm 10**	391 \pm 33**
6, 3 β -LCA	P2X2	n.d.	77 \pm 1.0*	55 \pm 7.5**	42 \pm 5.2**
	P2X4	n.d.	116 \pm 5.0	137 \pm 16*	142 \pm 7.2*
7, 3-Oxo-LCA	P2X2	n.d.	95 \pm 3.8	60 \pm 6.3*	53 \pm 12**
	P2X4	n.d.	118 \pm 10	149 \pm 8.7*	176 \pm 23*
8, 3-OAc-LCA	P2X2	167 \pm 8.4**	180 \pm 12**	193 \pm 15**	254 \pm 22**
	P2X4	157 \pm 12**	164 \pm 8.0**	202 \pm 22**	243 \pm 23**
9, 5 α -LCA	P2X2	n.d.	88 \pm 5.6	87 \pm 5.6	84 \pm 3.4*
	P2X4	n.d.	103 \pm 2.5	107 \pm 4.4	118 \pm 5.2
10, 3 β -Hydroxy-5 α -cholanic acid	P2X2	n.d.	82 \pm 8.4	77 \pm 6.9*	63 \pm 6.0**
	P2X4	n.d.	96 \pm 12	111 \pm 2.3	113 \pm 5.5
11, 4-DA	P2X2	91 \pm 1.5	70 \pm 4.1**	59 \pm 5.0**	53 \pm 4.2**
	P2X4	117 \pm 4.0	153 \pm 7.4**	249 \pm 37**	357 \pm 84**
12, 3 β -Hydroxy-5- cholenoic acid	P2X2	n.d.	71 \pm 4.2	66 \pm 8.3	64 \pm 8.7*
	P2X4	n.d.	107 \pm 6.2	117 \pm 4.2	129 \pm 13
13, LCA-Me-ester	P2X2	n.d.	94 \pm 6.0	88 \pm 9.2	93 \pm 9.2
	P2X4	n.d.	106 \pm 3.7	116 \pm 7.8	117 \pm 2.6
14, Glycine-LCA	P2X2	n.d.	96 \pm 6.0	82 \pm 3.8	55 \pm 6.3**
	P2X4	n.d.	115 \pm 3.5	123 \pm 2.8	142 \pm 4.1*
15, 12-Oxo-5 β -cholanic acid	P2X2	n.d.	105 \pm 12	211 \pm 15**	229 \pm 45**
	P2X4	n.d.	142 \pm 9*	230 \pm 53**	233 \pm 37**
16, Obeticholic acid	P2X2	n.d.	101 \pm 9.1	123 \pm 6.0	114 \pm 11
	P2X4	n.d.	104 \pm 3.2	143 \pm 6.3*	182 \pm 21*

Experiments were performed on HEK293T cells stimulated with 1 μ M ATP in the presence or absence of 1, 3, 10 or 30 μ M bile acid. The data shown are the mean \pm SEM values (in %) from 3 to 30 cells recorded in 3–10 independent experiments from P2X2 and P2X4 transfected HEK293T cells. (*) $P < 0.05$, (**) $P < 0.01$ between responses in the presence and absence of bile acids; n.d, not determined.

sites.

The enhanced potency of lithocholic acid led us to focus on this compound for further mechanistic experiments.

3.3. Lithocholic acid allosterically modulates P2X2 and P2X4 receptor channel gating

To explore the molecular mechanism by which lithocholic acid regulates the activity of P2X receptors, we studied its effect on responses stimulated by different concentrations of ATP (Fig. 4). Whole-cell recordings from P2X2-transfected cells (Fig. 4A) showed that 10 μ M lithocholic acid shifted the ATP concentration-response curve to the right (Fig. 4C) and increased the ATP concentration producing half-maximal effect (EC_{50}) by 2.4-fold (control $EC_{50} = 3.1 \pm 0.3 \mu$ M; lithocholic acid $EC_{50} = 7.6 \pm 1.3 \mu$ M; $P < 0.01$) without significantly decreasing the maximum current amplitude at saturating (100 μ M) ATP concentration (control: 3.1 ± 0.4 nA; lithocholic acid: 2.8 ± 0.3 nA;

$n=5$, $P > 0.05$). In contrast, whole-cell recordings from P2X4-transfected cells (Fig. 4B) revealed that 10 μ M lithocholic acid shifted the ATP concentration-response curve to the left (Fig. 4D) and reduced the EC_{50} value by 2.5-fold (control $EC_{50} = 2.7 \pm 0.4 \mu$ M; lithocholic acid $EC_{50} = 1.1 \pm 0.2 \mu$ M; $P < 0.05$) without significantly changing the maximum current amplitude (control: 2.0 ± 0.17 nA; lithocholic acid: 2.6 ± 0.27 nA; $n=7$, $P > 0.05$).

Thus, lithocholic acid acts as allosteric modulator of P2X receptors, which inhibits P2X2 and potentiates P2X4 receptor channel gating.

3.4. Lithocholic acid reduces the rate of P2X4 receptor desensitization

We examined the effects of lithocholic acid on the rate of P2X4 receptor desensitization using a prolonged (40 s) application of 100 μ M ATP (Fig. 5). In control experiments, the P2X4 receptor was desensitized to 4.09 ± 0.66 % of the initial peak amplitude ($n = 11$) within 40 s (Fig. 5A, black trace, and Fig. 5E). In the presence of 10 μ M lithocholic

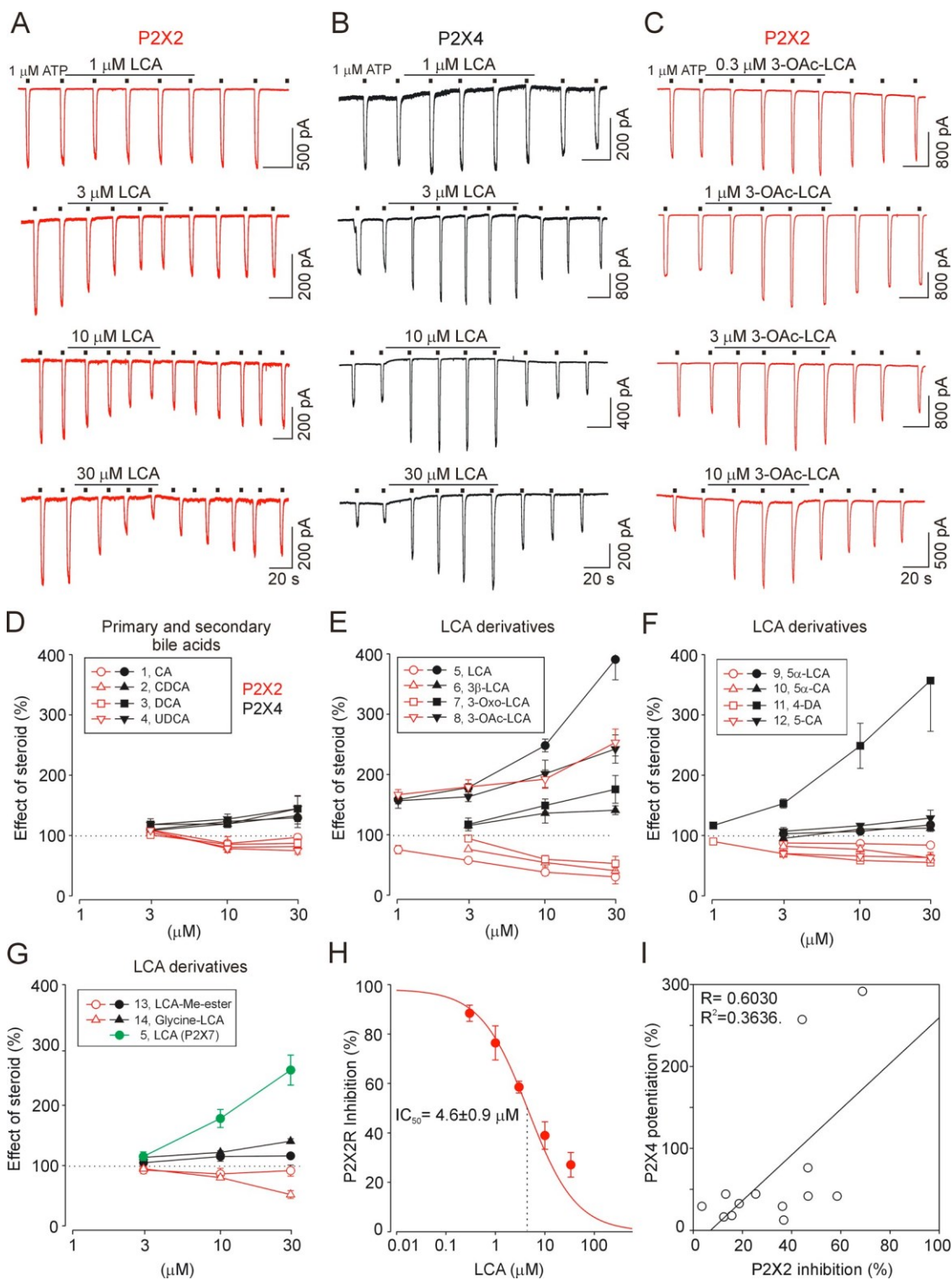


Fig. 3. Concentration-dependent effects of primary and secondary bile acids and lithocholic acid derivatives on P2X2, P2X4 and P2X7 receptor currents. (A) Example recordings from P2X2 receptor-expressing cells showing the inhibitory effects of several concentrations (1-30 μ M) of lithocholic acid (LCA) on 1 μ M ATP-induced responses. (B) Example recordings from P2X4 receptor-expressing cells showing the potentiating effects of several concentrations (1-30 μ M) of LCA on 1 μ M ATP-induced responses. (C) Example recordings from P2X2 receptor-expressing cells showing the potentiating effects of several concentrations (0.3-10 μ M) of 5 β -cholanic acid-3 α -yl acetate (3-OAc-LCA, compound **8**), on 1 μ M ATP-induced responses. (D) Concentration-dependent effects of primary and secondary bile acids (compounds **1** - **4**). (E) Concentration-dependent effects of lithocholic acid and its derivatives modified at position C-3 (compounds **5** - **8**). (F) Concentration-dependent effects of derivatives modified at position C-5 (compounds **9**-**12**). (G) Concentration-dependent effects of derivatives modified at position C-17 (compounds **13** - **14**) and concentration-dependent effect of LCA on 15 μ M BzATP-induced P2X7 responses (green). Data points represent the mean \pm SEM; n = 4 - 35 cells (from 3 - 12 passages) per concentration. (H) Concentration-dependent inhibitory effect of lithocholic acid on the peak amplitude of 1 μ M ATP-stimulated P2X2 current. The vertical dotted line indicates the concentration producing the 50 % inhibitory effect, and the number represents the mean IC₅₀ value. (I) Correlation between the inhibitory effect on P2X2 and potentiating effects on P2X4 currents for individual lithocholic acid analogues at 30 μ M.

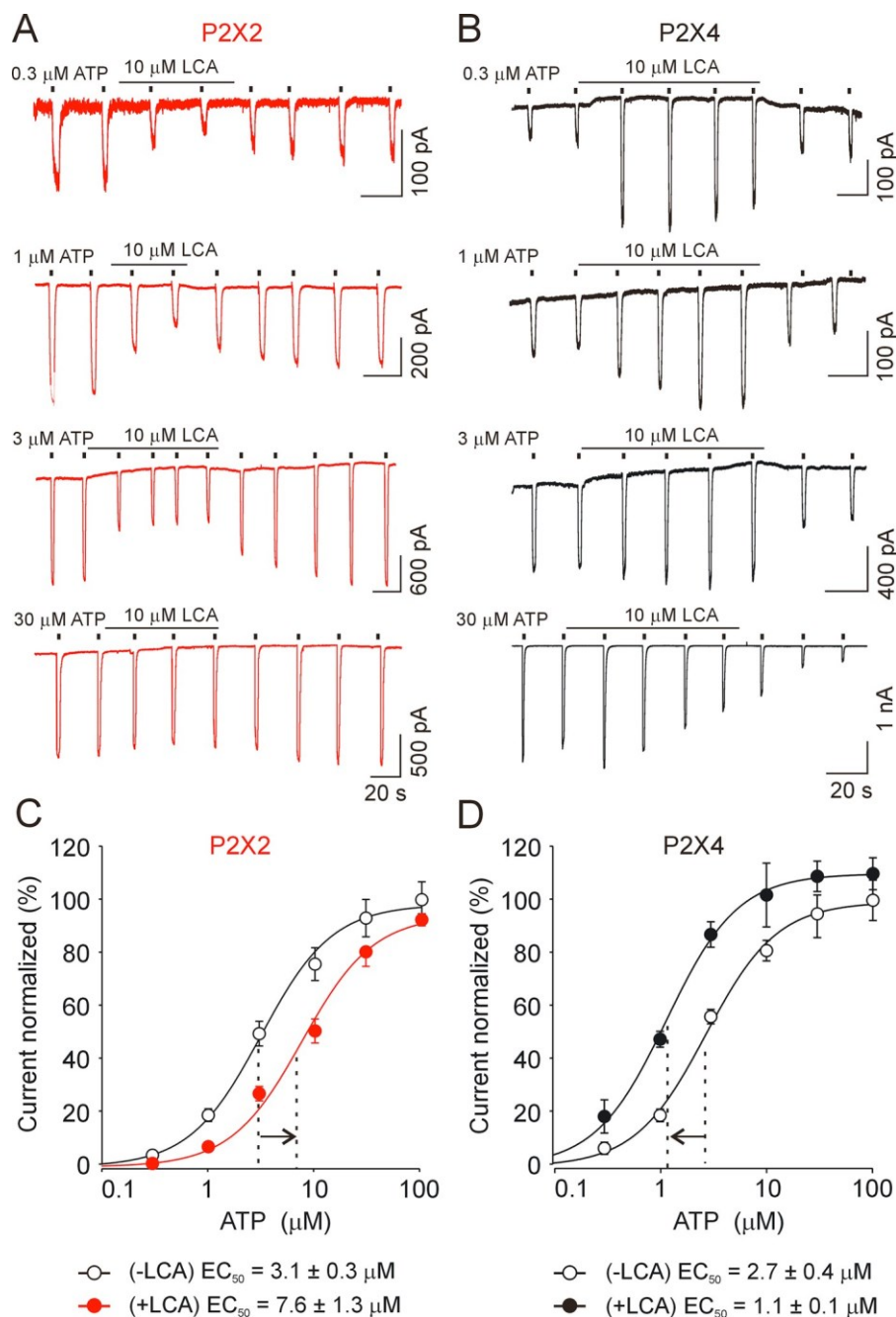


Fig. 4. ATP concentration-response curves for P2X2 and P2X4 receptors in the presence and absence of lithocholic acid. (A) Example recordings of responses to 0.3, 1, 3 and 30 μM ATP showing the inhibitory effect of 10 μM lithocholic acid (LCA) on the P2X2 receptor. (B) Example recordings of responses to 0.3, 1, 3 and 30 μM ATP showing the potentiating effect of 10 μM LCA on the P2X4 receptor. (C - D) Concentration-dependent effects of ATP on the peak amplitude of current in the absence (open circles) and presence (closed circles) of lithocholic acid for the P2X2 receptor (C) and P2X4 receptor (D). The vertical dotted lines represent the ATP concentration producing the 50 % maximal response, the arrows indicate the shift of the ATP concentration response curve in the presence of LCA, and the numbers represent the mean EC_{50} values in the presence (+LCA) and absence (-LCA) of lithocholic acid. The Hill coefficient was fixed to 1.3, a value obtained for the P2X4 receptor by fitting the curve in the absence of LCA. Data points represent the mean \pm SEM; n = 5-17 cells from 3-6 passages per concentration.

acid, the nondesensitized plateau current increased by 2.5-fold (to $10.5 \pm 1.5 \%$, n = 21; $P < 0.01$; Fig. 5A, gray trace, and Fig. 5E), and the desensitization time constant (τ_{des}) increased by 1.7-fold (control, $\tau_{des} = 7.2 \pm 0.45$ s, n = 11; lithocholic acid, $\tau_{des} = 12.0 \pm 1.2$ s, n = 21; $P < 0.01$; Fig. 5B).

When two or more consecutive ATP pulses were delivered, a small recovery of the peak current was observed after 60 s of washout in the control experiments (Fig. 5C), and the ratio of the 3rd peak to the 2nd peak current amplitude was 1.1 ± 0.1 (n = 12; Fig. 5F). Application of 10 μM lithocholic acid to the desensitized receptor potentiated the ATP-induced current so that the ratio of the 3rd peak to the 2nd peak current amplitude increased to 2.2 ± 0.4 (n = 7; Fig. 5F).

Based on these results, lithocholic acid reduces the rate of P2X4 receptor desensitization and increases the nondesensitized plateau similarly to ivermectin, a P2X4 receptor-specific allosteric modulator [39,40].

3.5. Antagonizing effects of lithocholic acid on the ivermectin-induced delay in P2X4 receptor deactivation

Ivermectin is well known to greatly prolong the deactivation kinetics of P2X4 receptor [33,39]. Previously, we showed that testosterone derivatives potentiate ATP-induced responses mediated by both P2X2 and P2X4 receptors and inhibit the ivermectin-induced prolongation of deactivation in P2X4 receptor channels [18]. Here, we measured P2X4 receptor deactivation in the presence and absence of lithocholic acid (10 μM) and ivermectin (3 μM) to investigate the ability of lithocholic acid to produce similar effect. The deactivation time constant (τ_{off}) was obtained by fitting the current decay evoked by 1 μM ATP removal. Lithocholic acid (10 μM) alone exhibited no effect on P2X4 deactivation (control: 286 ± 53 ms, n = 6, lithocholic acid: 355 ± 63 ms, n = 6, $P > 0.05$). Application of 3 μM ivermectin in the absence of lithocholic acid increased the amplitude of the 1 μM ATP-

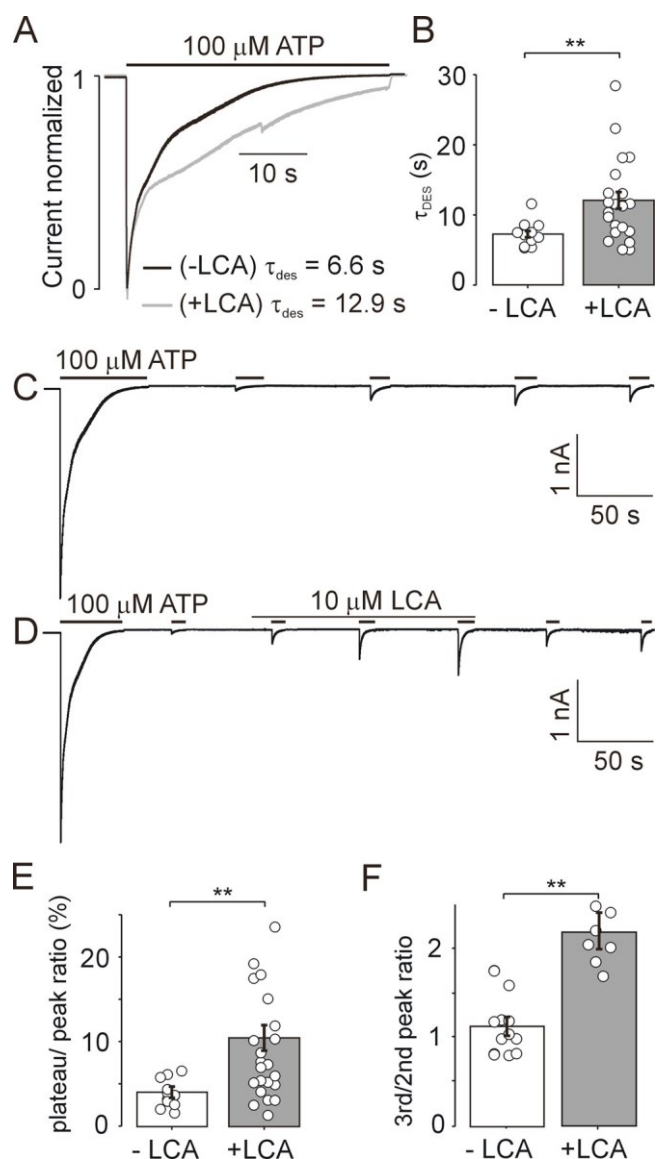


Fig. 5. Effects of lithocholic acid on the desensitization and resensitization properties of the P2X4 receptor. (A) Comparison of the time courses of currents induced by prolonged (40 s) application of 100 μ M ATP in the presence (gray trace) and absence (black trace) of 10 μ M lithocholic acid (LCA). The desensitization time constants (τ_{des}) were derived by fitting the curve to a biexponential function. (B) Summary histogram showing the means τ_{des} in the presence (gray column) and absence (white column) of 10 μ M LCA. Data are presented as the mean \pm SEM with a scatter plot of the individual data points ($n = 11$ -21 cells from 4 passages). (C) Representative recording showing the desensitization of the peak P2X4 receptor current induced by 100 μ M ATP and its recovery in control experiments. (D) Potentiation of recovery of ATP-induced current after application of 10 μ M LCA. (E) Summary histogram showing the level of desensitization (plateau-to-peak ratio) in the presence (gray column) and absence (white column) of LCA. (F) Summary histogram showing the recovery from desensitization (the 2nd to 3rd peak ratio) in control experiments (white column) and after LCA application (gray column). Data are presented as the mean \pm SEM with a scatter plot of the individual data points ($n = 7$ -21 cells from 4 passages). The statistical significance was estimated using the unpaired t-test, $P < 0.01$ (**).

induced P2X4 current by 8.5 ± 1.0 -fold (from 0.259 ± 0.032 nA to 2.2 ± 0.26 nA; $n=20$, $P < 0.01$), and the τ_{off} increased to 8.08 ± 0.69 s ($n = 20$; Fig. 6A). When ivermectin was applied in the presence of lithocholic acid, which alone increased the amplitude of the ATP-stimulated current by 2.5 ± 0.1 -fold (Fig. 3C), the amplitude of the ATP

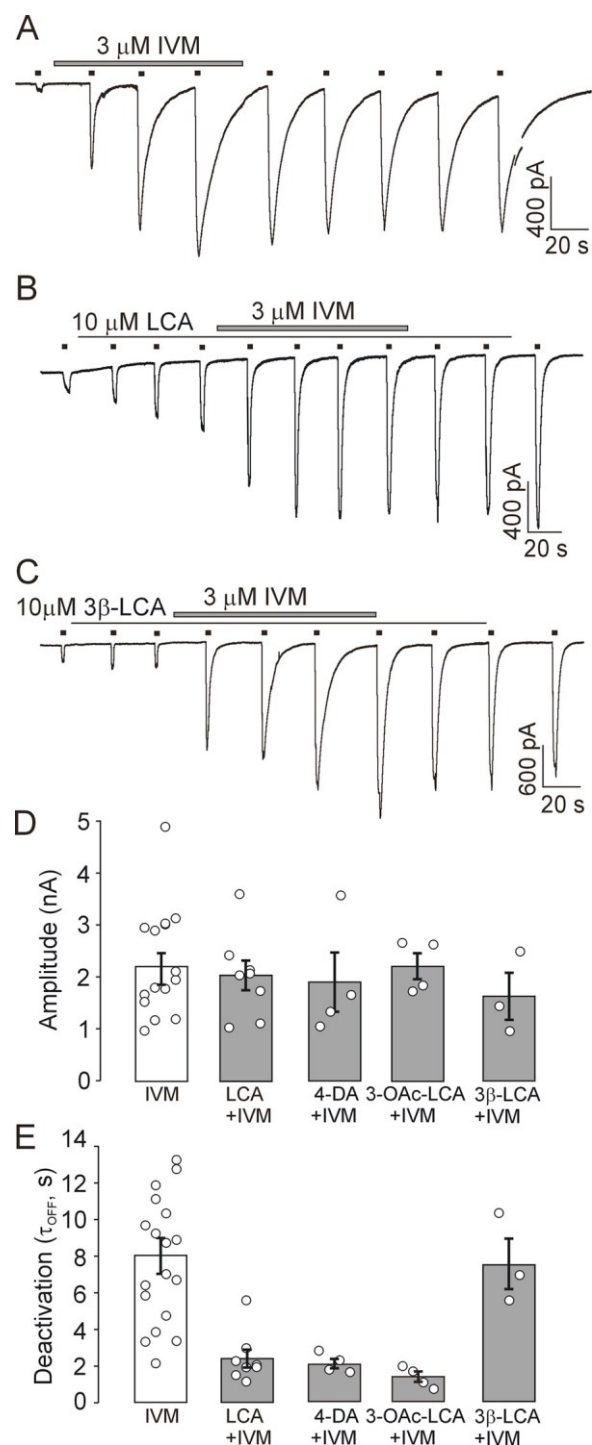


Fig. 6. Effects of lithocholic acid and its derivatives on ivermectin-induced delay in P2X4 receptor deactivation. (A) Example recording showing the effects of 3 μ M ivermectin (IVM) on 1 μ M ATP-induced current amplitude and channel deactivation. (B) Example recording showing the inhibitory effects of pretreatment with 10 μ M lithocholic acid (LCA) on IVM-induced delay in deactivation. (C) Example recording showing the lack of effects of pretreatment with 10 μ M isolithocholic acid (3 β -LCA) on IVM-induced delay in deactivation. (D - E) Summary histograms showing the effects of LCA, 4-dafachronic acid (4-DA), 5 β -cholanic acid-3 α -yl acetate (3-OAc-LCA), 4-DA and 3 β -LCA (all 10 μ M) on the 1 μ M ATP-induced current amplitude (D) and deactivation time constant (E) potentiated by 3 μ M IVM. Data are presented as the mean \pm SEM with a scatter plot of the individual data points ($n = 3$ -18 cells from 5-8 passages).

response was further increased by 5.2 ± 0.9 -fold (to 2.0 ± 0.28 nA; $n = 8$, $P < 0.01$; Fig. 6B and D), and the τ_{off} increased to only 2.41 ± 0.49 s ($n = 8$; Fig. 6E). A similar effect on ivermectin-induced deactivation was observed in the presence of 4-dafachronic acid and 5 β -cholanic acid-3 α -yl acetate (compound **8**), which potentiates both P2X2 and P2X4 receptors (Fig. 6E), but not in the presence of isolithocholic acid, which inhibits P2X2 but exhibits no significant potentiating effect on the P2X4 receptor (Fig. 6C and E).

These results showed that lithocholic acid and derivatives that significantly potentiate P2X4 receptor prevent ivermectin-induced delay in receptor deactivation, suggesting interaction with the ivermectin binding site.

3.6. Alanine scanning of the upper part of transmembrane domain-1

In the rat P2X4 receptor, mutations of Tyr42, Val43, Trp46, Val47 and Trp50 in the upper region of transmembrane domain-1 (TM1) have been shown to lower ivermectin occupancy [33,41–43], and mutations of Gly45 and Phe48 increase the ivermectin response [34,41]. To test a hypothesis that lithocholic acid interacts with ivermectin binding site, we examined sensitivity of alanine substitutions of all residues in the upper part of TM1 (from Tyr42 to Trp50) to 3 μ M lithocholic acid. The results of these investigations are summarized in Table S1 and Fig. 7.

We found that the potentiation effect of lithocholic acid was inhibited in Y42A mutant and significantly reduced in F48A and V43A mutants (Fig. 7A). Remaining receptors (I44A, G45A, W46A, V47A and W50A) were potentiated similarly to WT receptor (Fig. 7B). The V49A receptor was nonfunctional [44].

These results showed that modulatory sites for lithocholic acid and ivermectin could partly overlap at the P2X4 receptor (Fig. 7C).

3.7. Modulation of endogenously expressed P2X receptors in pituitary cells and hypothalamic neurons by lithocholic acid

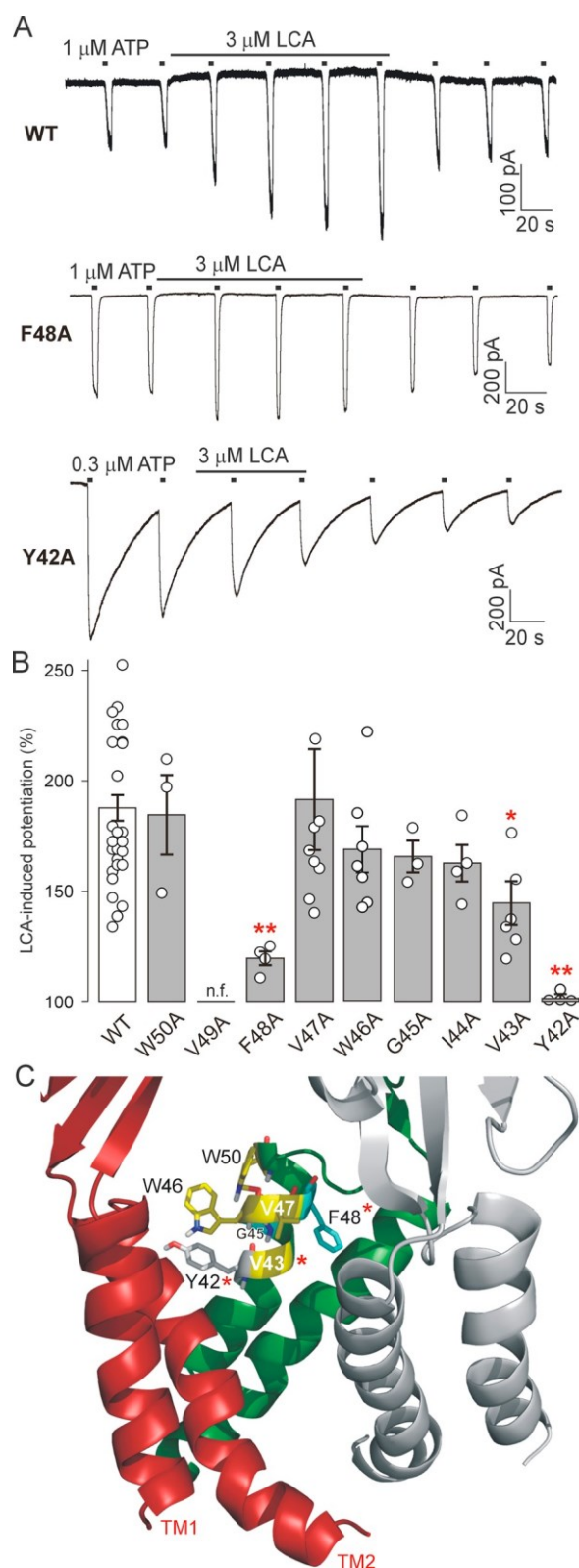
For comparison with endogenously expressed P2X receptors, the effects of lithocholic acid were tested in primary cultures of anterior pituitary cells and hypothalamic SON neurons in rat brain slices (Fig. 8). ATP-induced currents were recorded from identified pituitary gonadotrophs that express functional P2X2 receptors [45], non-identified pituitary cells that most probably express the P2X4 subtype [46,47], and SON neurons expressing both P2X2 and P2X4 subtypes [35]. The application of lithocholic acid (3–10 μ M) induced significant inhibition of the 100 μ M ATP-evoked currents in pituitary gonadotrophs, on average, to 85 ± 21 % (control: 64.2 ± 16.1 pA; LCA: 54.9 ± 14.0 pA; $n = 7$, $P < 0.05$; Fig. 8A and D), and potentiation of 50 μ M ATP-evoked currents in nonidentified pituitary cells, on average, to 137 ± 33 % (control: 16.0 ± 8.1 pA; LCA: 21.9 ± 14.0 pA; $n = 4$, $P < 0.05$; Fig. 8B, upper trace). In SON neurons (Fig. 8C), lithocholic acid (10 μ M) had a tendency to increase the amplitude of the ATP-induced current SON neurons, but this effect was not significant (Fig. 8F).

For comparison with other endogenously expressed ligand-gated ion channels, the effects of lithocholic acid on GABA-induced responses was subsequently investigated in nonidentified pituitary cells that all express the GABA(A) receptor [48]. In contrast to ATP-induced responses, the amplitude of the GABA-evoked current was inhibited on average to 72 ± 5.3 % (control: 163 ± 70 pA; lithocholic acid: 112 ± 49 pA; $n = 5$, $P < 0.05$; Fig. 8B, lower trace, and E).

Thus, lithocholic acid inhibits endogenously expressed P2X2 and GABA(A) receptors, and potentiates P2X4 receptor in pituitary cells, but no effect was observed in hypothalamic neurons expressing both P2X2 and P2X4 receptors.

4. Discussion

The results of our study show that low micromolar (1–3 μ M)



(caption on next page)

concentrations of lithocholic acid and its structural analog 4-dafachronic acid inhibit P2X2 and potentiate the P2X4 receptor without affecting the P2X7 subtype. Other principal bile acids exhibited no or reduced effects only at higher concentrations (10–30 μ M). In both P2X2 and P2X4 receptors, lithocholic acid shifts the ATP concentration-response curve and modulates ATP sensitivity but not efficacy. These

Fig. 7. Alanine-scanning mutagenesis and structural determinants for binding of lithocholic acid at the upper half of TM1 in P2X4 receptor. (A) Example recordings from cells expressing the rat P2X4 receptor wild type (WT) or transmembrane domain-1 (TM1) alanine mutants F48A and Y42A. All receptors were stimulated with 1 μM ATP pulse (2 s) in the presence or absence of lithocholic acids (LCA), except gain of function Y42A mutant that was stimulated with 0.3 μM ATP. (B) Summary graph showing the effects of LCA on the amplitude of ATP-induced current in WT and mutants in the upper part of TM1 (Y42A-W50A). Alanine mutant of Val49 was nonfunctional (n.f.) [44]. (C) Structural model of rat P2X4 receptor in open state with predicted TM1 part of ivermectin (IVM) binding site located between two neighboring subunits. It has been shown previously that mutations in Trp50, Trp46, Val47 and Val43 (yellow) abolish the IVM response, whereas mutations in Phe48 and Gly45 (cyan) increase the IVM response, and the lack of effects of IVM on mutation in Tyr42 (gray) reflects the inability of the receptor to be modified by IVM [33,34,41–43]. Red asterisks indicate amino acid residues showing altered sensitivity to LCA. Homology model of the rat P2X4 receptor was build previously [44] using the model of the zfp2X4.1R in the open (4DW1) state [9]. This figure was generated using Pymol v0.99 (<http://www.pymol.org>).

compounds also change the pharmacological properties of the P2X4 receptor and antagonize the effect of ivermectin on P2X4 receptor deactivation.

The higher potency of secondary bile acids to modulate P2X receptor activity might be due to the nonpolar character of these derivatives [26]. However, it has been reported that the potencies of common bile acids to modulate NMDA and GABA(A) receptors correlate with their affinities for albumin but not with lipophilicity [30], indicating a direct action at receptor channel proteins. Thus, upon binding, lithocholic acid acts as an allosteric modulator that may

change the P2X receptor protein conformation and subsequently alter the binding of orthosteric ligands, inhibiting or potentiating receptor function.

Multiple parts of the lithocholic acid molecule seem to be involved in the interaction with the P2X receptor protein, since modifications at C-3, C-5 or COOH abolished both the potentiating and inhibitory effects to varying degrees. Summary Fig. 9 shows that the most efficient were modifications of COOH group and modifications at position C-5, with the exception of dafachronic acid, which is a natural bile acid. Modifications at position C-3 revealed an interesting properties of compounds **8** as compared with other compounds considering the trend of the ability to modulate differently P2X2 vs P2X4 receptors. This compound potentiated both receptors and we hypothesized that the 3 α -hydroxy group might be a pharmacophore that define the ability of the molecule to switch between potentiation and inhibition. In agreement with this hypothesis, compound **15** that also lacks 3 α -hydroxy group potentiated both P2X2 and P2X4 receptors. On the other hand, compound **7** is also lacking free hydroxyl group while maintaining the switch between potentiation and inhibition. Then, we could speculate that compound **8** as compared with compound **7** bears more sterically demanding group that may not fit the potential binding site.

Because our results show that the inhibitory effects on P2X2 do not clearly correlate with the potentiating effects on P2X4 for individual derivatives, the differential modulation could be attributed to the presence of two distinct modulatory sites. Accumulating evidence supports that other steroids also exhibit both positive or negative allosteric modulatory effects on P2X2 and P2X4 receptors. For example, dehydroepiandrosterone (DHEA) selectively potentiates an agonist response of endogenously expressed P2X2 receptors in cultured rat sensory

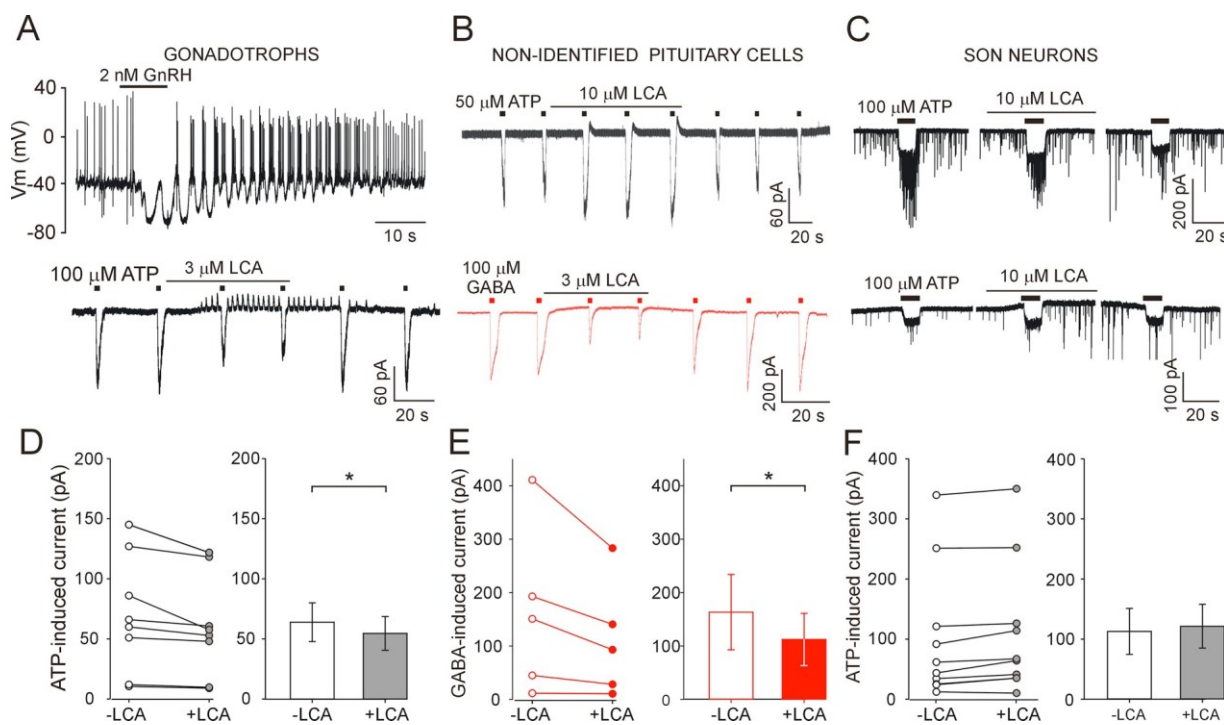


Fig. 8. Effects of lithocholic acid on endogenously expressed P2X receptors in anterior pituitary cells and hypothalamic neurons. (A) On top is an example of the current clamp whole-cell recording of electrical activity in gonadotrophs stimulated by gonadotropin-releasing hormone (GnRH) that was used to identify these cells. Below shows that the application of lithocholic acid (LCA, 3 μM) inhibited the ATP (100 μM)-stimulated response mediated by native P2X2 receptors in gonadotrophs voltage clamped at -60 mV. Residual membrane potential oscillations are due to oscillatory Ca^{2+} -dependent K^{+} currents previously activated by GnRH. (B) On top shows potentiating effect of 10 μM LCA on the 50 μM ATP-induced current in nonidentified anterior pituitary cells. Below shows the inhibitory effect of 3 μM LCA on GABA (50 μM)-induced current in nonidentified pituitary cells. (C) Example recordings from two SON neurons in rat brain slices showing the effect of 10 μM LCA on the 50 μM ATP-induced current. (D - F) Summary graphs showing the effects of LCA on the amplitude of ATP-induced current in pituitary gonadotrophs (D), amplitude of GABA-induced current in nonidentified pituitary cells (E), and amplitude of ATP-induced current in SON neurons (F). Data are presented as the mean \pm SEM with a scatter plot of the individual data points (ATP, $n = 8$ cells from 3 cell culture preparations; GABA, $n = 7$ cells from 3 cell culture preparations). Significant differences between responses in the presence and absence of LCA were estimated using a paired t-test, $P < 0.05$ (*).

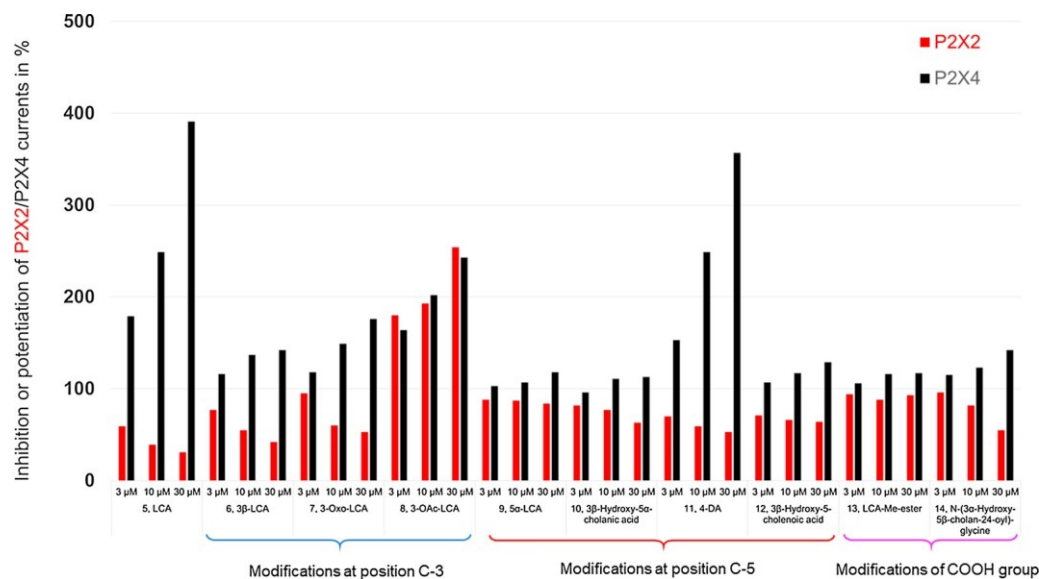


Fig. 9. Summary figure illustrating the structure-activity relationship data for lithocholic acid derivatives.

neurons [16]. Synthetic neurosteroids, such as alfaxalone and allo-pregnanolone, and THDOC (3 α ,21-dihydroxy-5 β -pregnan-20-one), a metabolite of deoxycorticosterone, potentiate while very high concentrations of pregnanolone inhibit the activity of P2X4 receptors expressed in HEK293 or oocyte cells [17]. Previously, we showed that testosterone derivatives potentiate both P2X2 and P2X4 receptors expressed in HEK293 cells [18]. Thus, interpretation of our data in the context of earlier studies suggests that there might be two different binding sites for steroids in the structure of P2X receptors.

Lithocholic acid potentiates the P2X4 receptor by a molecular mechanism that is similar to that of ivermectin, a P2X4 receptor-specific allosteric modulator [33,39,40], and antagonizes the effect of ivermectin on P2X4 receptor channel deactivation, suggesting that it might interact with the ivermectin binding site. The structure of the ivermectin-bound P2X4 receptor channel is still unsolved, but so far data indicate that ivermectin binds between two neighboring subunits within the transmembrane helices in the upper part of transmembrane domain of the P2X4 receptor [33,41,42]. Here we show that three of seven previously identified ivermectin hits in the upper part of the TM1 contribute also to recognition of lithocholic acid molecule at the P2X4 receptor. Together, these data strongly indicate that the binding site for bile steroids allosterically potentiating the P2X4 receptor might overlap with the ivermectin binding site.

Despite the receptor-specific effects of ivermectin, the binding site for potentiating steroids is likely conserved among P2X2 and P2X4 receptors. Our previous data revealed that the potencies of testosterone derivatives clearly correlate for these two types of P2X receptors [18], and the present data also show that compound **8** potentiates the P2X2 and P2X4 receptors equally. Whether the binding site for steroids producing inhibitory effects is also conserved and where it is localized is an interesting question that remains to be solved in further studies.

The P2X receptors are known to be modulated differently by endogenous cholesterol. For example, cholesterol depletion inhibits the P2X1 and P2X4 receptor function when expressed in HEK293 cells [49,50] but not P2X2 or P2X3 receptor function [50,51]. ATP concentration-response curves for P2X4 receptor were not significantly different between control and cholesterol depleted cells [51]. Thus, the mechanism underlying suppression of P2X4 by cholesterol depletion does not involve modulation of intrinsic channel properties and it is therefore unlikely that cholesterol binding site might play a role in modulation of P2X4 receptor by lithocholic acid. The P2X7 receptor is also known to be modulated by endogenous cholesterol that inhibits

channel activity within the transmembrane helices [21,23], and drugs that interact with the cholesterol binding site of P2X7 may reduce the inhibitory effects of cholesterol [22]. Lithocholic acid at a moderate concentration (10 μ M) significantly potentiates the BzATP-induced current, indicating that it might interact with the cholesterol binding site of the P2X7 receptor.

During our work on this manuscript, two studies aiming to describe the effects of bile acids on P2X receptors expressed in oocytes have been published [31,32], and the results of these studies are partially contradictory. Schmid et al. (2019) found that the rat P2X2 receptor is strongly inhibited by 20 μ M taurine-conjugated lithocholic acid, hydroxycholeic acid and chenodeoxycholeic acid, whereas other P2X receptors (P2X1, P2X3, P2X4 and P2X7) were only mildly affected and the human P2X2 receptor was potentiated [31]. Ilyaskin et al. (2019) used 250 μ M taurine-conjugated bile acids and reported that application of either conjugated or unconjugated deoxycholeic acid causes strong inhibition of the human P2X4 receptor, while chenodeoxycholeic and cholic acids did not significantly alter P2X4-mediated currents [32]. Our present study is consistent with the report by Schmid et al. (2019) showing that lithocholic acid inhibits the rat P2X2 receptor and is also consistent with the report by Ilyaskin et al. (2019) showing that secondary bile acids are more potent than primary bile acids. However, inhibition of the P2X4 receptor was not observed. Instead, we show here for the first time that lithocholic acid is an effective positive allosteric modulator of the rat P2X4 receptor. Overall, the results of previous studies and our study suggest that the modulatory effect of bile acids on P2X receptors is complex and needs further investigation.

Bile acids might regulate P2X2 and P2X4 receptor-controlled processes not only in places where they are synthesized (liver and gut), but also in other parts of the body, that might receive bile acids from peripheral circulation. Primary bile acids are synthesized in the liver, secreted into the duodenum via bile, reabsorbed in the ileum and circulated back to the liver via the portal vein [52]. Lithocholic acid is formed from chenodeoxycholeic acid only under anaerobic conditions by bacterial action in the colon, and its major metabolite in humans is isolithocholic acid [53]. During this so-called enterohepatic circulation, approximately 3% of the total bile acids remain in the gut at very high concentrations (approximately 200–1000 μ M) [54]. The concentration of bile acids in the portal vein is 10–80 μ M and that in systemic circulation is approximately 2–10 μ M [55]. Lithocholic acid inhibits the P2X2 receptor with an IC₅₀ of 4.6 \pm 0.9 μ M, clearly indicating that P2X receptors might be modulated well below these physiological

concentrations.

In the liver, P2X4 is predominant among P2 receptor subtypes [56]. A study on P2X4 knockout (KO) mice showed that ATP signaling through P2X4 contribute to liver repair after acute injury [56], and modulate fibrotic liver repair during chronic injury [57]. ATP is present in a concentration of approximately 1.5 μM in human bile [58], where it stimulates a biliary epithelial cell secretory response by activating the P2Y [59,60] and possibly also the P2X4 receptors [61,62]. Our findings indicate that bile acids might potentiate all these P2X4 receptor-controlled processes in liver.

P2X2 receptor immunoreactivity [63,64] and transcripts of the P2X4 receptor [65] have been detected in the colon. Lithocholic acid is hepatotoxic, and there is increasing evidence that it is involved in the carcinogenesis of different organs, including the colon and liver [66,67]. Our findings indicate that tumor-promoting action of lithocholic acid might potentially involve modulation of P2X receptors.

Bile acids can also be detected in the brains of humans and rodents [68,69]. Although the origin of brain bile acids is unclear, the principal source is apparently peripheral circulation [26]. Bile acids may modify neuronal activity and thereby brain function by acting as inhibitors of GABA(A) and NMDA receptors [30,70]. Here, we show that lithocholic acid inhibits ATP-induced responses mediated by the P2X2 receptor in pituitary gonadotrophs and potentiates P2X4 responses in other pituitary cells, but has no effect on ATP-induced responses in SON neurons expressing both P2X2 and P2X4 receptors [35,71], suggesting that these receptors could complement their function.

Bile acids have been reported to be protective against neurodegeneration [26]. Twenty bile acids have been identified in the rat brain [68]. Quantification of bile acid metabolites measured in the plasma of patients suffering from Alzheimer's disease identified lithocholic acid as a putative biomarker in this disease [72]. There is abundant evidence correlating the overexpression of P2X receptors to neurodegenerative diseases, including Alzheimer's disease [73,74], and it has been found that P2X2 [73] and P2X4 protein levels [75] were increased in hippocampal neurons exposed to the A β peptide. Thus, it is possible that lithocholic acid could modulate the P2X2 and P2X4 receptor-controlled toxic processes under pathological conditions, for example in Alzheimer's disease.

Recent findings suggest that ivermectin mediates alcohol intake, sensorimotor gating and dopamine-induced motor behaviour through modulation of P2X4 receptors [76–78]. Ivermectin also possesses a potential anti-cancer effect: it kills breast cancer cells through potentiating P2X4/P2X7 signaling [79]. Whether lithocholic acid and related molecules, that could be endogenous ligands for the ivermectin site, regulate these processes remains to be clarified in further studies.

Our data also show that 4-dafachronic acid exhibits almost identical effects as lithocholic acid. Dafachronic acid is a natural bile acid, but little is known about its physiological role. Endogenous dafachronic acid has been reported to be an important steroid hormone in the development of *Caenorhabditis elegans* and the parasitic nematode *Haemonchus contortus* [80], and in killifish [81]. It is not unreasonable to speculate that in mammals, the gut microbiota could generate such a bile acid starting with lithocholic acid and that 4-dafachronic acid might also play a role in circulating signaling molecules.

5. Conclusion

We screened primary and secondary bile acids, synthesized new derivatives and structural analogues of lithocholic acid, and identified lithocholic acid and dafachronic acid as the most effective bile acids that allosterically inhibit P2X2 and potentiate P2X4 receptor gating. The alanine-scanning mutagenesis of the upper part of transmembrane domain-1 revealed that lithocholic acid could interact with ivermectin binding site. These results indicate that lithocholic acid is a bioactive steroid that may help to further unveil the importance of P2X2 and P2X4 receptors in many physiological processes, including gut

homeostasis, carcinogenesis and neurodegeneration.

CRedit authorship contribution statement

Sonja Sivcev: Investigation, Data curation. **Barbora Slavikova:** Investigation, Data curation. **Milorad Ivetic:** Investigation. **Michal Knezu:** Investigation. **Eva Kudova:** Conceptualization, Resources, Visualization, Supervision, Writing - review & editing. **Hana Zemkova:** Conceptualization, Investigation, Visualization, Supervision, Writing - review & editing.

Declaration of Competing Interest

None.

Acknowledgments

This work was supported by grants from the The Czech Science Foundation (GA CR, grant #18-05413S), Charles University Grant Agency (grants #928517 and #918120), the Ministry of Education, Youth and Sports of the Czech Republic within the LQ1604 National Sustainability Program II (Project BIOCEV-FAR) and the project BIOCEV (CZ.1.05/1.1.00/02.0109), and by the Academy of Sciences of the Czech Republic (RVO 61388963).

The preliminary data for this article were presented as a poster P-263 at conference EFMC International Symposium on Advances in Synthetic and Medicinal Chemistry, Athens, Greece, September 1-5, 2019, <https://www.efmc-asmc.org/>

Appendix A. Supplementary data

Supplementary material related to this article can be found, in the online version, at doi:<https://doi.org/10.1016/j.jsbmb.2020.105725>.

References

- [1] R.A. North, Molecular physiology of P2X receptors, *Physiol. Rev.* 82 (2002) 1013–1067.
- [2] A. Nicke, H.G. Baumert, J. Rettinger, A. Eichele, G. Lambrecht, E. Mutschler, G. Schmalzing, P2X1 and P2X3 receptors form stable trimers: a novel structural motif of ligand-gated ion channels, *EMBO J.* 17 (1998) 3016–3028.
- [3] S. Valera, N. Hussy, R.J. Evans, N. Adami, R.A. North, A. Surprenant, G. Buell, A new class of ligand-gated ion channel defined by P2X receptor for extracellular ATP, *Nature* 371 (1994) 516–519.
- [4] G.E. Torres, T.M. Egan, M.M. Voigt, Identification of a domain involved in ATP-gated ionotropic receptor subunit assembly, *J. Biol. Chem.* 274 (1999) 22359–22365.
- [5] S. Ennion, S. Hagan, R.J. Evans, The role of positively charged amino acids in ATP recognition by human P2X(1) receptors, *J. Biol. Chem.* 275 (2000) 29361–29367.
- [6] L.H. Jiang, F. Rassendren, A. Surprenant, R.A. North, Identification of amino acid residues contributing to the ATP-binding site of a purinergic P2X receptor, *J. Biol. Chem.* 275 (2000) 34190–34196.
- [7] C. Coddou, Z. Yan, T. Obsil, J.P. Huidobro-Toro, S.S. Stojilkovic, Activation and regulation of purinergic P2X receptor channels, *Pharmacol. Rev.* 63 (2011) 641–683.
- [8] T. Kawate, J.C. Michel, W.T. Birdsong, E. Gouaux, Crystal structure of the ATP-gated P2X(4) ion channel in the closed state, *Nature* 460 (2009) 592–598.
- [9] M. Hattori, E. Gouaux, Molecular mechanism of ATP binding and ion channel activation in P2X receptors, *Nature* 485 (2012) 207–212.
- [10] R.J. Evans, Orthosteric and allosteric binding sites of P2X receptors, *Eur. Biophys. J.* 38 (2009) 319–327.
- [11] C. Coddou, S.S. Stojilkovic, J.P. Huidobro-Toro, Allosteric modulation of ATP-gated P2X receptor channels, *Rev. Neurosci.* 22 (2011) 335–354.
- [12] C.E. Muller, Medicinal chemistry of P2X receptors: allosteric modulators, *Curr. Med. Chem.* 22 (2015) 929–941.
- [13] A.R. Ase, N.S. Honson, H. Zaghdane, T.A. Pfeifer, P. Seguela, Identification and characterization of a selective allosteric antagonist of human P2X4 receptor channels, *Mol. Pharmacol.* 87 (2015) 606–616.
- [14] Z. Yan, A. Khadra, A. Sherman, S.S. Stojilkovic, Calcium-dependent block of P2X7 receptor channel function is allosteric, *J. Gen. Physiol.* 138 (2011) 437–452.
- [15] H. Xu, B. Wu, F. Jiang, S. Xiong, B. Zhang, G. Li, S. Liu, Y. Gao, C. Xu, G. Tu, H. Peng, S. Liang, H. Xiong, High fatty acids modulate P2X(7) expression and IL-6 release via the p38 MAPK pathway in PC12 cells, *Brain Res. Bull.* 94 (2013) 63–70.
- [16] M. De Roo, J.L. Rodeau, R. Schlichter, Dehydroepiandrosterone potentiates native

- ionotropic ATP receptors containing the P2X2 subunit in rat sensory neurones, *J. Physiol. (Paris)* 552 (2003) 59–71.
- [17] J.F. Codocedo, F.E. Rodriguez, J.P. Huidobro-Toro, Neurosteroids differentially modulate P2X ATP-gated channels through non-genomic interactions, *J. Neurochem.* 110 (2009) 734–744.
- [18] S. Sivcev, B. Slavikova, M. Rupert, M. Ivetic, M. Nekarodova, E. Kudova, H. Zemkova, Synthetic testosterone derivatives modulate rat P2X2 and P2X4 receptor channel gating, *J. Neurochem.* 150 (2019) 28–43.
- [19] E.E. Baulieu, Neurosteroids: a novel function of the brain, *Psychoneuroendocrinology* 23 (1998) 963–987.
- [20] Y. Hojo, S. Kawato, Neurosteroids in adult Hippocampus of male and female rodents: biosynthesis and actions of sex steroids, *Front. Endocrinol. (Lausanne)* 9 (2018) 183.
- [21] L.E. Robinson, M. Shridhar, P. Smith, R.D. Murrell-Lagnado, Plasma membrane cholesterol as a regulator of human and rodent P2X7 receptor activation and sensitization, *J. Biol. Chem.* 289 (2014) 31983–31994.
- [22] R.D. Murrell-Lagnado, Regulation of P2X purinergic receptor signaling by cholesterol, *Curr. Top. Membr.* 80 (2017) 211–232.
- [23] A. Karasawa, K. Michalski, P. Mikhelzon, T. Kawate, The P2X7 receptor forms a dye-permeable pore independent of its intracellular domain but dependent on membrane lipid composition, *eLife* 6 (2017).
- [24] A.M. Dopico, A.N. Bukiya, Regulation of Ca(2+)-Sensitive K(+) channels by cholesterol and bile acids via distinct channel subunits and sites, *Curr. Top. Membr.* 80 (2017) 53–93.
- [25] I. Alimov, S. Menon, N. Cochran, R. Maher, Q. Wang, J. Alford, J.B. Concannon, Z. Yang, E. Harrington, L. Llamas, A. Lindeman, G. Hoffman, T. Schuhmann, C. Russ, J. Reece-Hoyes, S.M. Canham, X. Cai, Bile acid analogues are activators of pyrin inflammasome, *J. Biol. Chem.* 294 (2019) 3359–3366.
- [26] Y. Kiriya, H. Nochi, The Biosynthesis, Signaling, and neurological functions of bile acids, *Biomolecules* 9 (2019).
- [27] K.D. Setchell, A.M. Lawson, N. Tanida, J. Sjoval, General methods for the analysis of metabolic profiles of bile acids and related compounds in feces, *J. Lipid Res.* 24 (1983) 1085–1100.
- [28] A.N. Bukiya, J.E. McMillan, A.L. Fedinec, S.A. Patil, D.D. Miller, C.W. Leffler, A.M. Parrill, A.M. Dopico, Cerebrovascular dilation via selective targeting of the cholane steroid-recognition site in the BK channel beta1-subunit by a novel non-steroidal agent, *Mol. Pharmacol.* 83 (2013) 1030–1044.
- [29] A.M. Dopico, M.T. Kirber, J.J. Singer, J.V. Walsh Jr., Membrane stretch directly activates large conductance Ca(2+)-activated K+ channels in mesenteric artery smooth muscle cells, *Am. J. Hypertens.* 7 (1994) 82–89.
- [30] S.R. Schubring, W. Fleischer, J.S. Lin, H.L. Haas, O.A. Sergeeva, The bile steroid chenodeoxycholate is a potent antagonist at NMDA and GABA(A) receptors, *Neurosci. Lett.* 506 (2012) 322–326.
- [31] A. Schmidt, S. Jousen, R. Hausmann, S. Grunder, D. Wiemuth, Bile acids are potent inhibitors of rat P2X2 receptors, *Purinergic Signal.* 15 (2019) 213–221.
- [32] A.V. Ilyashin, F. Sure, V. Nesterov, S. Haerteis, C. Korbmayer, Bile acids inhibit human purinergic receptor P2X4 in a heterologous expression system, *J. Gen. Physiol.* 151 (2019) 820–833.
- [33] I. Jelinkova, Z. Yan, Z. Liang, S. Moonat, J. Teisinger, S.S. Stojilkovic, H. Zemkova, Identification of P2X(4) receptor-specific residues contributing to the ivermectin effects on channel deactivation, *Biochem. Biophys. Res. Commun.* 349 (2006) 619–625.
- [34] H. Zemkova, A. Khadra, M.B. Rokic, V. Tvrdonova, A. Sherman, S.S. Stojilkovic, Allosteric regulation of the P2X4 receptor channel pore dilation, *Pflugers Arch.* 467 (2015) 713–726.
- [35] V. Vavra, A. Bhattacharya, H. Zemkova, Facilitation of glutamate and GABA release by P2X receptor activation in supraoptic neurons from freshly isolated rat brain slices, *Neuroscience* 188 (2011) 1–12.
- [36] H. Zemkova, J. Vanecek, Differences in gonadotropin-releasing hormone-induced calcium signaling between melatonin-sensitive and melatonin-insensitive neonatal rat gonadotrophs, *Endocrinology* 141 (2000) 1017–1026.
- [37] S.J. Fountain, R.A. North, A C-terminal lysine that controls human P2X4 receptor desensitization, *J. Biol. Chem.* 281 (2006) 15044–15049.
- [38] Y.D. Wang, W.D. Chen, D.D. Moore, W. Huang, FXR: a metabolic regulator and cell protector, *Cell Res.* 18 (2008) 1087–1095.
- [39] B.S. Khakh, W.R. Proctor, T.V. Dunwiddie, C. Labarca, H.A. Lester, Allosteric control of gating and kinetics at P2X(4) receptor channels, *J. Neurosci.* 19 (1999) 7289–7299.
- [40] L. Mackay, H. Zemkova, S.S. Stojilkovic, A. Sherman, A. Khadra, Deciphering the regulation of P2X4 receptor channel gating by ivermectin using Markov models, *PLoS Comput. Biol.* 13 (2017) e1005643.
- [41] I. Jelinkova, V. Vavra, M. Jindrichova, T. Obsil, H.W. Zemkova, H. Zemkova, S.S. Stojilkovic, Identification of P2X(4) receptor transmembrane residues contributing to channel gating and interaction with ivermectin, *Pflugers Arch.* 456 (2008) 939–950.
- [42] S.D. Silberberg, M. Li, K.J. Swartz, Ivermectin interaction with transmembrane helices reveals widespread rearrangements during opening of P2X receptor channels, *Neuron* 54 (2007) 263–274.
- [43] M. Popova, J. Trudell, K. Li, R. Alkana, D. Davies, L. Asatryan, Tryptophan 46 is a site for ethanol and ivermectin action in P2X4 receptors, *Purinergic Signal.* 9 (2013) 621–632.
- [44] M.B. Rokic, S.S. Stojilkovic, V. Vavra, P. Kuzyk, V. Tvrdonova, H. Zemkova, Multiple roles of the extracellular vestibule amino acid residues in the function of the rat P2X4 receptor, *PLoS One* 8 (2013) e59411.
- [45] H. Zemkova, A. Balik, Y. Jiang, K. Kretschmannova, S.S. Stojilkovic, Roles of purinergic P2X receptors as pacemaking channels and modulators of calcium-mobilizing pathway in pituitary gonadotrophs, *Mol. Endocrinol.* 20 (2006) 1423–1436.
- [46] H. Zemkova, M. Kucka, S. Li, A.E. Gonzalez-Iglesias, M. Tomic, S.S. Stojilkovic, Characterization of purinergic P2X4 receptor channels expressed in anterior pituitary cells, *Am. J. Physiol. Endocrinol. Metab.* 298 (2010) E644–651.
- [47] W. Zhao, Y. Zhang, R. Ji, G.E. Knight, G. Burnstock, H. Yuan, Z. Xiang, Expression of P2X receptors in the rat anterior pituitary, *Purinergic Signal.* (2019).
- [48] H.W. Zemkova, I. Bjelobaba, M. Tomic, H. Zemkova, S.S. Stojilkovic, Molecular, pharmacological and functional properties of GABA(A) receptors in anterior pituitary cells, *J. Physiol. (Lond.)* 586 (2008) 3097–3111.
- [49] C. Vial, R.J. Evans, Disruption of lipid rafts inhibits P2X1 receptor-mediated currents and arterial vasoconstriction, *J. Biol. Chem.* 280 (2005) 30705–30711.
- [50] R.C. Allsopp, U. Lalo, R.J. Evans, Lipid raft association and cholesterol sensitivity of P2X1–4 receptors for ATP: chimeras and point mutants identify intracellular amino-terminal residues involved in lipid regulation of P2X1 receptors, *J. Biol. Chem.* 285 (2010) 32770–32777.
- [51] J. Li, S.J. Fountain, Fluvastatin suppresses native and recombinant human P2X4 receptor function, *Purinergic Signal.* 8 (2012) 311–316.
- [52] A. Wahlstrom, S.I. Sayin, H.U. Marschall, F. Backhed, Intestinal crosstalk between bile acids and microbiota and its impact on host metabolism, *Cell Metab.* 24 (2016) 41–50.
- [53] M.I. Kelsey, S.A. Sexton, The biosynthesis of ethyl esters of lithocholic acid and isolithocholic acid by rat intestinal microflora, *J. Steroid Biochem.* 7 (1976) 641–647.
- [54] J.P. Hamilton, G. Xie, J.P. Raufman, S. Hogan, T.L. Griffin, C.A. Packard, D.A. Chatfield, L.R. Hagey, J.H. Steinbach, A.F. Hofmann, Human cecal bile acids: concentration and spectrum, *American journal of physiology, Gastrointestinal and liver physiology* 293 (2007) G256–263.
- [55] T.Q. de Aguiar Vallim, E.J. Tarling, P.A. Edwards, Pleiotropic roles of bile acids in metabolism, *Cell Metab.* 17 (2013) 657–669.
- [56] A. Besnard, J. Gautherot, B. Julien, A. Tebbi, I. Garcin, I. Doignon, N. Pean, E. Gonzales, D. Cassio, B. Grosse, B. Liu, H. Safya, F. Cauchois, L. Humbert, D. Rainteau, T. Tordjmann, The P2X4 purinergic receptor impacts liver regeneration after partial hepatectomy in mice through the regulation of biliary homeostasis, *Hepatology* 64 (2016) 941–953.
- [57] C. Le Guilcher, I. Garcin, O. Dellis, F. Cauchois, A. Tebbi, I. Doignon, C. Guettier, B. Julien, T. Tordjmann, The P2X4 purinergic receptor regulates hepatic myofibroblast activation during liver fibrogenesis, *J. Hepatol.* 69 (2018) 644–653.
- [58] R.S. Chari, S.M. Schutz, J.E. Haebig, G.H. Shimokura, P.B. Cotton, J.G. Fitz, W.C. Meyers, Adenosine nucleotides in bile, *Am. J. Physiol.* 270 (1996) G246–252.
- [59] T. Schlenker, J.M. Romac, A.I. Sharara, R.M. Roman, S.J. Kim, N. LaRusso, R.A. Liddle, J.G. Fitz, Regulation of biliary secretion through apical purinergic receptors in cultured rat cholangiocytes, *Am. J. Physiol.* 273 (1997) G1108–1117.
- [60] A.K. Dutta, A.K. Khimji, M. Sathe, C. Kresge, V. Parameswara, V. Esser, D.C. Rockey, A.P. Feranchak, Identification and functional characterization of the intermediate-conductance Ca(2+)-activated K(+) channel (IK-1) in biliary epithelium, *American journal of physiology, Gastrointestinal and liver physiology* 297 (2009) G1009–1018.
- [61] R.B. Doctor, T. Matzakos, R. McWilliams, S. Johnson, A.P. Feranchak, J.G. Fitz, Purinergic regulation of cholangiocyte secretion: identification of a novel role for P2X receptors, *American journal of physiology, Gastrointestinal and liver physiology* 288 (2005) G779–786.
- [62] D.S. Emmett, A. Feranchak, G. Kilic, L. Puljak, B. Miller, S. Dolovcak, R. McWilliams, R.B. Doctor, J.G. Fitz, Characterization of ionotropic purinergic receptors in hepatocytes, *Hepatology* 47 (2008) 698–705.
- [63] W. Guo, Q.Q. Sui, X.F. Gao, J.F. Feng, J. Zhu, C. He, G.E. Knight, G. Burnstock, Z. Xiang, Co-localization of P2r protein and P2X2 receptors in the mouse enteric nervous system, *Purinergic Signal.* 12 (2016) 489–496.
- [64] P. Castelucci, H.L. Robbins, J.B. Furness, P2X(2) purine receptor immunoreactivity of intraganglionic laminar endings in the mouse gastrointestinal tract, *Cell Tissue Res.* 312 (2003) 167–174.
- [65] J. Tanaka, M. Murate, C.Z. Wang, S. Seino, T. Iwanaga, Cellular distribution of the P2X4 ATP receptor mRNA in the brain and non-neuronal organs of rats, *Arch. Histol. Cytol.* 59 (1996) 485–490.
- [66] V. Kozoni, G. Tsioulis, S. Shiff, B. Rigas, The effect of lithocholic acid on proliferation and apoptosis during the early stages of colon carcinogenesis: differential effect on apoptosis in the presence of a colon carcinogen, *Carcinogenesis* 21 (2000) 999–1005.
- [67] A.A. Goldberg, A. Beach, G.F. Davies, T.A. Harkness, A. Leblanc, V.I. Titorenko, Lithocholic bile acid selectively kills neuroblastoma cells, while sparing normal neuronal cells, *Oncotarget* 2 (2011) 761–782.
- [68] X. Zheng, T. Chen, A. Zhao, X. Wang, G. Xie, F. Huang, J. Liu, Q. Zhao, S. Wang, C. Wang, M. Zhou, J. Panee, Z. He, W. Jia, The brain metabolome of male rats across the lifespan, *Sci. Rep.* 6 (2016) 24125.
- [69] N. Mano, T. Goto, M. Uchida, K. Nishimura, M. Ando, N. Kobayashi, J. Goto, Presence of protein-bound unconjugated bile acids in the cytoplasmic fraction of rat brain, *J. Lipid Res.* 45 (2004) 295–300.
- [70] Y. Yanovsky, S.R. Schubring, Q. Yao, Y. Zhao, S. Li, A. May, H.L. Haas, J.S. Lin, O.A. Sergeeva, Waking action of ursodeoxycholic acid (UDCA) involves histamine and GABA receptor block, *PLoS One* 7 (2012) e42512.
- [71] M. Ivetic, A. Bhattacharyya, H. Zemkova, P2X2 receptor expression and function is upregulated in the rat supraoptic nucleus stimulated through refeeding after fasting, *Front. Cell. Neurosci.* 13 (2019) 284.
- [72] J. Marksteiner, I. Blasko, G. Kemmler, T. Koal, C. Humpel, Bile acid quantification of 20 plasma metabolites identifies lithocholic acid as a putative biomarker in Alzheimer's disease, *Metabolomics* 14 (2018) 1.

- [73] F. Saez-Orellana, M.C. Fuentes-Fuentes, P.A. Godoy, T. Silva-Grecchi, J.D. Panes, L. Guzman, G.E. Yevenes, J. Gavilan, T.M. Egan, L.G. Aguayo, J. Fuentealba, P2X receptor overexpression induced by soluble oligomers of amyloid beta peptide potentiates synaptic failure and neuronal dyshomeostasis in cellular models of Alzheimer's disease, *Neuropharmacology* 128 (2018) 366–378.
- [74] P.A. Godoy, O. Ramirez-Molina, J. Fuentealba, Exploring the role of P2X receptors in alzheimer's disease, *Front. Pharmacol.* 10 (2019) 1330.
- [75] R. Varma, Y. Chai, J. Troncoso, J. Gu, H. Xing, S.S. Stojilkovic, M.P. Mattson, N.J. Haughey, Amyloid-beta induces a caspase-mediated cleavage of P2X4 to promote purinotoxicity, *Neuromolecular Med.* 11 (2009) 63–75.
- [76] M. Bortolato, M.M. Yardley, S. Khoja, S.C. Godar, L. Asatryan, D.A. Finn, R.L. Alkana, S.G. Louie, D.L. Davies, Pharmacological insights into the role of P2X4 receptors in behavioural regulation: lessons from ivermectin, *Int. J. Neuropsychopharmacol.* 16 (2013) 1059–1070.
- [77] K.M. Franklin, S.R. Hauser, A.W. Lasek, R.L. Bell, W.J. McBride, Involvement of purinergic P2X4 receptors in alcohol intake of high-alcohol-Drinking (HAD) rats, *Alcohol. Clin. Exp. Res.* 39 (2015) 2022–2031.
- [78] S. Khoja, V. Shah, D. Garcia, L. Asatryan, M.W. Jakowec, D.L. Davies, Role of purinergic P2X4 receptors in regulating striatal dopamine homeostasis and dependent behaviors, *J. Neurochem.* 139 (2016) 134–148.
- [79] D. Draganov, S. Gopalakrishna-Pillai, Y.R. Chen, N. Zuckerman, S. Moeller, C. Wang, D. Ann, P.P. Lee, Modulation of P2X4/P2X7/Pannexin-1 sensitivity to extracellular ATP via Ivermectin induces a non-apoptotic and inflammatory form of cancer cell death, *Sci. Rep.* 5 (2015) 16222.
- [80] G. Ma, T. Wang, P.K. Korhonen, N.D. Young, S. Nie, C.S. Ang, N.A. Williamson, G.E. Reid, R.B. Gasser, Dafachronic acid promotes larval development in *Haemonchus contortus* by modulating dauer signalling and lipid metabolism, *PLoS Pathog.* 15 (2019) e1007960.
- [81] A.L.T. Romney, E.M. Davis, M.M. Corona, J.T. Wagner, J.E. Podrabsky, Temperature-dependent vitamin D signaling regulates developmental trajectory associated with diapause in an annual killifish, *Proc. Natl. Acad. Sci. U.S.A.* 115 (2018) 12763–12768.